THE DYNAMICS OF LEVITATED DROPS IN AN ELECTRIC FIELD

E.H. Trinh, R.G. Holt, and D.B. Thiessen[1]
Jet propulsion Laboratory
California Institute of Technology

ABSTRACT

Ultrasonic and electrostatic levitation techniques have allowed the experimental investigation of the nonlinear oscillatory dynamics of free droplets with diameter between 0.1 and 0.4 cm. The measurement of the resonance frequencies of the first three normal modes of large amplitude shape oscillations in an electric field of varying magnitude has been carried out with and without surface charges for weakly conducting liquids in air. These oscillations of nonspherical levitated drops have been driven by either modulating the ultrasonic field or by using a time-varying electric field, and the free decay from the oscillatory state has been recorded. A decrease in the resonance frequency of the driven fundamental quadruple mode has been measured for increasing oblate deformation in the absence of an electric field. Similarly, a decrease in this frequency has also been found for increasing DC electric field magnitude. A soft nonlinearity exists in the amplitude dependence of the resonant mode frequencies for freely decaying as well as ultrasonically and electrically driven uncharged drops. This decrease in resonance frequency is accentuated by the presence of free surface charge on the drop. Subharmonic resonance excitation has been observed for drops in a time-varying electric field, and hysteresis exists for resonant modes driven to large amplitude. Mode coupling from lower-order resonances to higher-order modes has been found to be very weak, *even* for fairly large amplitude shape oscillations. Most of these results are in general agreement with predictions from recent analytical and numerical investigations.

[1] Now at the Department of Physics, Washington State University, Pullman, WA

1. INTRODUCTION

The dynamics of isolated and freely suspended drops are of fundamental interest because of their inherent nonlinear characteristics, but also because of the practical need for an understanding of the governing physical mechanisms in natural and industrial processes involving disperse two-phase systems. In particular, evidence has been obtained indicating that the induction of drop shape oscillations can lead to an enhancement of mass and heat transfer. This is relevant to applications in industrial processes involving solvent extraction and direct contact heat exchangers[1-3]. At the same time, progress in levitation technology has introduced the possibility of investigating the properties of materials in the liquid state under conditions only obtainable for levitated samples [4-6]. In this context, the accuracy of measurements of the surface properties of acoustically, electrostatically, or electromagnetically levitated melts depends on our knowledge of the often nonlinear dynamics of the droplets. An understanding of the levitation field effects on the drop response is also required to interpret the associated experimental observations. Although the small amplitude shape oscillations of totally free and spherical liquid drops are well understood, they are very seldom applicable to actual Earth-based physical systems. The need for a theoretical understanding of large amplitude oscillations of deformed drops thus provides the motivation for the rigorous and detailed measurement of their characteristics.

The large amplitude shape oscillations of isolated free drops have been extensively examined in recent years, although the emphasis of the theoretical work has been mainly on inviscid or weakly viscous liquids. A great deal of insight on the dynamics of free droplets has been gained in the initial oscillatory phase [7] as well as in the asymptotic driven stead y state and free decay stages[7-13]. Thus, over the past two decade, an impressive array of investigations using both analytical and numerical techniques has addressed the problem of axisymmetric large amplitude oscillations of inviscid drops, and partial corroboration with experimental findings has been obtained 14-15 . *More* recently, however, nonlinear treatments of viscous drop oscillations have been proposed [16,17] , and their predictions have been favorably compared with experimental results based on the observations of drops detached from a nozzle and freely falling under the influence of gravity and aerodynamic drag.

From the available evidence to date, the salient and widely accepted nonlinear characteristic appears to be the decrease in resonance frequency of the fundamental shape oscillation mode with increasing *oscillation amplitude.* In this case, both analytical and numerical methods predict a quadratic dependence of the frequency on the oscillation amplitude. Experimental results obtained using acoustically levitated droplets in an immiscible host 14 as well as data from free droplets falling in air [15] are in general agreement with these theoretical predictions. Another finding is that the inclusion of significant viscosity in the numerical simulations of 1 arge amplitude free decaying drop dynamics reduces the imbalance between the time durations of the oblate and prolate configurations for the fundamental mode, and it prevents resonant mode coupling predicted by inviscid theoretical treatments, Numerical modelling has also suggested that the initial configuration of the droplet influences its subsequent dynamical behavior in the free decay phase [16] .

The work described in this paper deals with the experimental study of small and large amplitude shape oscillations of single low-viscosity drops acoustically levitated in air and in the presence of a constant or time-varying electric field. Although some results based on low gravity experiments carried out in space will be discussed, the bulk of the discussion concerns free drops levitated on Earth. The shape altering capabilities associated with *combined acoustic and electrostatic levitation* must therefore be taken into account when a comparison is made between theoretical predictions and experimental findings. This subtle field-drop interaction is the primary motivation for this investigation, A parallel experimental study of the oscillations of bubbles and drops immersed in a liquid has also been carried out concurrently, and the results are reported elsewhere 18.

Published theoretical treatments have addressed the equilibrium shape and stability of charged and uncharged drops in an electric field. Son ıe of the earlier analytical work was performed by Taylor [19] and Brazier-Smith et al. 20 by assuming a spheroidal shape for the drop. The result was a reasonably accurate evaluation of the equilibrium shape and of the natural resonance frequencies. Numerical computations have also been carried out by Miksis 21, Adornato and Brown [22], Basaran and Striven [23], and Pelekasis and Tsamopoulos 24 for the equilibrium shape. Tsamopoulos and Brown 25, Tsamopoulos, Akylas, and Brown [26], Natarajan and Brown 27, Feng and Beard 28 , and Kang 29, have theoretically studied the effects of electric fields and charges on shape oscillations, the resonant modes coupling process, and the break-up of charged drops in electric fields.

More recently, Feng and Leal [30] have formulated a numerical code to investigate the static shape and nonlinear oscillations of drops in both static and time-periodic electric fields.

It appears that a substantial theoretical foundation for the understanding of the dynamics of charged and uncharged conducting drop in electric fields has been laid. In this paper, we wish to describe experimental results which can be compared with some of the theoretical predictions advanced in the publications mentioned above.

The physical system of interest is a free, single-phase liquid droplet of low viscosity surrounded by a gaseous medium at rest. The drop can carry a free surface electrical charge with magnitude varying between zero and the Rayleigh limit, and it can be conducting or insulating. The primary scientific interest is in the dynamic response of the drop to an excitation by time-varying ultrasonic and/or electric stress fields: steady-state driven as well as free decaying shape oscillations are to be examined to characterize the resonant response. The drop will therefore be under the influence of both acoustic radiation pressure and electrical forces. In the Earth's gravitational field, the initial equilibrium shape of a levitated drop will be primarily determined by its surface tension and by the ultrasonic field intensity in the absence of an electric field. The static and dynamic effects of the electric field will thus be quantified relative to the equilibrium oblate shaped drop determined by the ultrasonic stress distribution over the drop surface. This reference state can also be experimentally examined by setting the electric field to zero.

The following sections of the paper will deal first with a discussion of the experimental approach. Results of the measurement of the equilibrium shape of levitated drops as a function of the absolute and relative magnitude of the electric and ultrasonic fields will be reported next to show how the geometry of a levitated drop can be continuously controlled. The dependence of the resonance frequency of the fundamental (or quadrupolar) mode of shape oscillation on the static deformation from the perfect spherical geometry in the absence of an electric field will follow. The effect of a static electric field on the resonance frequencies of shape oscillations of charged and uncharged drops has also been measured, and the findings will be described , and finally, the outcome of a study of the dynamic response of levitated drops to both ultrasonic and electric fields drive will be presented to show nonlinear characteristics such as subharmonic excitation, soft nonlinearity in the resonance frequencies, and mode coupling.

2. EXPERIMENTAL APPROACH

2.1 Levitation Apparatus

The 'single-axis' ultrasonic levitator has been previously used for the investigation of the physics of free droplets on Earth as well as in low gravity 4.31-3[5]. Similarly, previous use of the electrostatic levitator has allowed the experimental investigation of the statics and dynamics of levitated charged drops [36-38] having diameters in the sub-millimeter to millimeter range. In this particular contribution, we combine the two methods to investigate the effects of electric field stresses on the surface of ultrasonically levitated drops carrying an electric charge of *variable* magnitude in the full range of drop stability between the Taylor (high field intensity, no surface charge) and Rayleigh limits (maximum surface charge in constant field). The current approach allows the levitation of *uncharged* drops while a previous electrostatic-acoustic hybrid levitation scheme was limited to the study of acoustically rotated and oscillated charged drops 38.

Figure 1 shows a schematic representation of the experimental apparatus. A drop is depicted as being levitated between the reflector and the radiating plate of the ultrasonic driver. The outer surface of the latter is grounded, while the reflector is connected to a high voltage, low current source effective from DC to about 1 kHz. A function generator and RF amplifier provide the driving signal for the ultrasonic levitator, while the high voltage amplifier and a second function generator control the electric field magnitude and frequency. These two systems can each control drop levitation and shape modulation independently or they can be used in a complementary mode. In the experiments described in this paper the sample was primarily ultrasonically levitated, and the electric field was used either to modulate or to control the static drop shape.

The voltage between the reflector and radiating plate, V_E, is a combination of a DC and of a low frequency sinusoidal signal:

$$V_E = V_{0E} + v_e \cos(\omega_e t), \qquad (1)$$

where V_{0E} is a DC voltage used for the electrostatic levitation of a charged drop, and v_e and ω_e are the amplitude and frequency of the AC component drive. of the electric field respectively. This time-varying component induces both a *static distortion* as well as *oscillatory shape changes* when $2\omega_e$ (ω_e for the case of sub-harmonic excitation) is close

to the value of *one* of the resonant shape mode frequencies (Feng and Beard, 1991 a)[28]. The electric field oriented parallel to the gravity vector, and the levitated drop is elongated along the direction of the electric field. In general, the electric force can be expressed by

$$\vec{F}_e = \rho_e \vec{E} - \frac{1}{2} E^2 \vec{\nabla} \varepsilon + \vec{\nabla} \left[\frac{1}{2} \left(\frac{\partial \varepsilon}{\partial \rho} \right)_T E \vec{E}^2 \right], \qquad (2)$$

where the first term is usual Coulomb force on a free charge ρ_e, the second term represents the force on an inhomogeneous dielectric in a field of magnitude E, and the last term describes the force on a dielectric in a non-uniform field. The electric force components involved in altering the drop shape both depend on the square of the electric field magnitude. For a field described by expression (1) they vary at both the frequencies ω_e and $2\omega_e$. When V_{OE}=0, the drop shape is thus modulated by the time-varying electric field at the frequency $2\omega_e$.

For an axisymmetric and inviscid spherical charged drop, Rayleigh's result[39] for the normal modes is

$$\omega_{lk}^2 = \frac{l(l-1)}{\rho R^3} \left[\sigma(l+2) - \frac{Q^2}{(4\pi)^2 \varepsilon_0 R^3} \right], \qquad (3)$$

where R is the drop radius, p its density, σ its surface tension, and ε_0 the permittivity of the surrounding medium (air in this case). The resonance frequencies are independent of the second index k which reflects non-spherically symmetric contributions not accounted for by Rayleigh's theory. As the experimental evidence presented below will show, this degeneracy is removed in actual levitated drops due to the non-spherical initial drop shape. For a more complete three-dimensional treatment, the drop shape is usually described in terms of the spherical harmonics (Landau and Lifshitz, 1959)[40] given by $Y_{lk}(\theta,\phi)=P_l^k(\cos\theta)e^{ik\phi}$. For each *l* there exists one axisymmetric oscillation mode and 1 *distinct* three-dimensional modes. Thus, for the fundamental *l*=2 mode, there are three distinct modes which are degenerate for the case of a spherical drop. This degeneracy is removed when the static equilibrium drop shape becomes non- spherical, and, in principle, three distinct resonance frequencies and oscillatory motion types can be measured. The axisymmetric mode (also called the "pulsation" mode) is described by the zonal harmonics (*k*=0); the other three-dimensional modes, sometimes called the "transverse-shear" (*k*=1)

and "toroidal" (k=2) modes, are described by the tesseral and sectorial harmonics respectively.

In addition to the direct excitation from the time-varying electric field, drop shape oscillations can also be driven by the modulation of the acoustic radiation force. In this case, the voltage accross the ultrasonic transducer, V_{ac}, is given by

$$V_{ac} = v_{ac0}\left[1 + M\cos(\omega_m t)\right]\cos(\omega_{ac} t), \qquad (4)$$

v_{ac0} is the amplitude of the carrier voltage at the frequency $\omega_{ac} = 2\pi f_{ac}$ for the acoustic standing wave (f_{ac} =24.6 kHz), M is the modulation index for the amplitude modulation of the acoustic force at the frequency ω_m. Because the acoustic radiation force is proportional to the square of the acoustic pressure, this force is therefore proportional to V^2_{ac}, and this amplitude modulation results in a time-varying acoustic force at both the frequencies ω_m as well as $2\omega_m$. This translates into a periodic *flattening* of the drop by the acoustic force, an action opposite to the periodic *elongation* of a liquid sample submitted to a time-varying electric field.

2.2 **The monitoring and imaging of drop oscillations**

The dynamic response of the levitated drop to either steady-state or transient excitation is recorded in two ways: the shadow of a laser-illuminated drop is monitored by a photodetector located behind a vertical slit, and the image of the backlit drop is recorded by a video camera at 30 frames/see or at high rates (2,000 or 4,000 frames/see). The temporal information is redundant, but the video image recording method allows complete shape analysis for *axisymmetric* oscillations, 'he photodetector output can be absolutely calibrated with respect to the real drop shape by comparing with the simultaneous y strobed illumination of the drop under steady-state oscillation drive. The strobing frequency is slaved to the oscillation drive frequency, but the strobe input signal phase can be vaned with respect to the low frequency oscillation drive signal. This phase is varied until an image for the maximum oscillation amplitude is obtained; this can be used for the absolute calibration by comparing the photodetector signal amplitude and the measured deformation on the drop image. The sequence of shapes characteristic of large amplitude oscillations in the fundamental l=2, k=0 mode shown in **figure** 2 has been obtained by video recording the drop shape under strobed illumination.

For the case of *axisymmetric* oscillations of a free drop, the usual expansion into the Legendre polynomials is used. The shape of the drop, described by $R(\theta,t)$ is

$$R(\theta,t) = R_0\left[1 + \sum_{l=2}^{l^*} \mathrm{Re}\left[c_l(t)P_l(\cos\theta)\right]\right], \qquad (5)$$

where R_0 is the radius of the sphere of the same volume equivalent to an undeformed drop, $P_l(\cos\theta)$ *is the* Legendre polynomial of degree *1,* and $c_l(t)$ are the coefficients describing the deformed drop shape in terms of the standard Legendre shapes. Implementing a method similar to that used by Becker et al. (199 1)[15], we digitize the contour of the deformed shapes from the high-speed video images recorded during drop oscillations, and fit the Legendre polynomials to the experimental edge coordinates. Using this method we can obtain the time series for each $c_l(t)$ for driven and freely decaying shape oscillations. For the data described in this paper, we have limited ourselves to $l^*=6$. A video frame digitally analyzed is not greater than **320x 240** pixels and up to 256 levels of gray.

At large amplitude oscillations and for non-spherical drops, non-axisymmetric normal modes couple to the desired axisymmetric oscillations, and this approach is no longer satisfactory for the analysis of the shape. The onset of non- axisymmemc motion is immediately reflected in a non-constant value for the "volume" that is calculated from the digitized image under the assumption of axial symmetry.

3. EXPERIMENTAL RESULTS

3.1 Static Shape of Ultrasonically Levitated Drops in an Electric Field

The static shape of ultrasonically levitated droplets in air and in the Earth gravitational field has been theoretically [41,42] and experimentally studied in the past [43,34,44]. The electrohydrodynamic deformation of drops in weakly conducting liquids has also been recently determined to essentially follow Taylor's leaky dielectric theory [45,46]. The shape of drops in a static uniform electric field for both conducting and insulating liquids has been investigated by O'Konski et al. (1953) [47,48] and Sample et al.(1970)[49]. In this study, however, we experimentally investigate the *superposition* of ultrasonic and electric stresses and their effects on the shape of levitated charged and uncharged drops in air. In terms of the equilibrium shape of a levitated drop, the oblate deformation caused by the ultrasonic

radiation stresses can be **"balanced" out by a** prolate-biased drop shaping due to an electric field. If both the ultrasonic and electric fields are **axisymmetric,** a resulting near-spherical shape can be experimentally obtained with the appropriate combination of acoustic pressure and electrode voltage.

A related problem has been investigated by Pruppacher et al.[50] (1982), and deals with the shape of aerodynamically supported droplets in a vertical wind tunnel and in the presence of a vertically directed electric field. The size of the droplets they investigated ranged between 0.05 and 0.3 cm equivalent spherical diameter (the diameter of the equivalent spherical drop of the same volume as the distorted suspended drop). In this case, the drop shape under terminal velocity conditions is determined by the combination of hydrodynamic and electric forces. In the absence of an electric field, the equilibrium shape of these drops is oblate, but inherently asymmetric: their cross section is flattened on the upstream side (lower hemisphere) and curved on the downstream side (upper hemisphere) due to the asymmetrical hydrodynamic stress distribution. For relatively larger droplet sizes (equivalent spherical diameter greater than 0.4 cm), the equilibrium shape of ultrasonically levitated drops is almost the opposite: The upper surface is flattened and the lower hemisphere is more highly curved. In roughly the same drop size range (0.05 to 0.3 cm equivalent spherical diameter), however, ultrasonically levitated droplets are nearly symmetrical with respect to the equator. On the other hand, the effect of the vertical electric field on the equilibrium drop shape, is qualitatively similar for both aerodynamically and ultrasonically levitated drops: electrical forces act opposite to hydrodynamic and ultrasonic forces, and they can be used to obtain a more spherical drop shape. More recent analytical results have been produced by Coquillat and Chauzy[51] (1993) for the combined effect of aerodynamic and electrical forces, and they have been favorably correlated with wind tunnel experimental results.

Figure 3 shows the results of measurements of the *equilibrium* geometrical aspect ratio a/b = $R(\theta=\pi/2) / R(\theta=0)$ of a 1.85 mm diameter ultrasonically levitated uncharged oblate water-glycerol solution drop as a function of the magnitude of the static electric field. The upper limit of the electric field intensity was determined by breakdown in the air gap separating the ultrasonic driver and the reflector. The three data sets correspond to three different acoustic pressure levels, and the drop never attains a spherical equilibrium shape even for the highest allowable electric field intensity. Spherical and prolate static drop shapes can be obtained for larger volumes as shown by **figure** 4 which reproduces a series of photographs of a 0.32 cm diameter water-glycerol drop for constant acoustic pressure

level but increasing electric field intensity. The gradual change from the oblate shape (a-c), to spherical (d), to symmetric prolate (e,f), and finally to asymmetric prolate (g, h) can be clearly observed in this series of photographs. In this case, the drop center of mass remains at a constant position because the drop does not carry any significant net surface charge. The loss of symmetry with respect to the drop equator has been theoretically predicted by Feng and Leal 30 (1995) for uncharged drops and high electric field intensity. These measurements have been obtained with droplets displaying *randomly oriented* residual rotation with angular velocity on the order of 1 rps. Such a rotation velocity would induce shape distortions of less than 0.5% for the material parameter range under consideration.

3.2 Shape oscillations Driven by Modulated Ultrasonic Radiation Force

32.1 Fundamental Resonance Frequency Variation with Static Drop Shape

The measurement of the *fundamental* mode resonant frequency of drops levitated in an immiscible liquid host to a modulation in the acoustic radiation force has been used in the past to yield results consistent with the linear theory [52,53]. The results of the same Earth-based measurements using drops levitated in a gaseous host medium have been difficult to interpret because of effects of the static distortion from the spherical shape, and of drop rotation. Not only has a shift in the resonance frequency from the value predicted by linear theory been documented [54,55], but a split of the resonance frequency of driven oscillations into three characteristic values has also been found 4 This shift and splitting of the fundamental resonance frequency has also been measured for *rotating* drops levitated in an immiscible liquid host [56], and it has been theoretically explained by analyzing the role of the Coriolis force 57. It appears from the available evidence that a rigorous measurement of the resonance frequency in the small-amplitude range of shape oscillations must account for the static shape, the field-induced restoring forces, as well as the rotational state of the drop. We report here the results of the measurement of the fundamental resonance mode frequency of *small-amplitude driven* shape oscillations for non-rotating drops as a function of the oblate deformation.

The control of unwanted drop rotation in a single-axis ultrasonic levitator can be achieved by using a variety of empirical methods which vary according to the specific levitator configuration. There is no agreed-upon theoretical account for the generation of this torque, but existing evidence points to the contributing role of acoustically-induced

streaming 58. In the particular case reported here, a low gravity environment appeared to eliminate the unwanted drop rotation by allowing a substantial reduction of the acoustic intensity required for drop levitation. The measurements were carried out in a NASA KC-135 airplane flying parabolic trajectories and providing 15 to 20 second periods of effective reduced gravity (down to about 0.05 to 0.01 g, g being the Earth gravitational acceleration at sea level) 59. Many measurements have been carried out over a period of 8 years, but the results presented here consist of five sets of data for five different drops obtained during four different series of airplane flight experiments. The selection of these five sets was based on the following criteria: The oscillations were *axisymmetric* (i.e. $l=2$, $k=0$ in equation (3)), the rate of drop rotation was less than 0.1 rps, the amplitude of translational instability was less than 10% of the drop effective equilibrium diameter, and the reference frequency for a "spherical" drop shape ($0.99 < a/b < 1.1$) was obtained for each measurement of the frequency at a different a/b parameter (where a/b is the ratio Of the horizontal to vertical dimensions).

The measurement of the resonance frequency was carried out in the following manner. A drop was levitated during level flight (effective gravity level of about 1 g) and the ultrasonic transducer power was adjusted to allow the levitation of the drop in the climbing and recovery phases of the parabolic trajectory (up to 1.8 g). At this stage, the drop is drastically flattened because of the high sound intensity. During the low gravity period, the transducer power was reduced to a minimum level necessary to position the drop and to adjust its shape to near-spherical . The driven resonance frequency was then measured by maximizing the amplitude of the oscillatory response of the drop to a varying modulation of the acoustic force. The amplitude of the shape oscillations was always kept at values below 10% of the vertical drop dimension (less than 10% of the effective drop radius). The drop response was visually monitored and the mode shape ($l=2, k=0$) was identified using the magnified drop image from a video camera equipped with a microscope lens. The modulation frequency at maximum response was measured to within 0.1 Hz for the low viscosity (1 to 3 cP) liquids and drop sizes used (0.3 to 0.4 cm diameter). The aspect ratio of the oblate shaped drops was measured by digitizing the video recorded images which were absolutely calibrated by imaging a ball hewing of roughly the same size as the drops. A reference measurement of the resonance frequency for a near-spherical drop was always taken in the high-to-low gravity cycle right after the one during which a measurement at higher deformation had been recorded. The relative shift in the resonance frequency for a specific aspect ratio (or deformed drop shape) is the ratio of the values of these two consecutive measurements. The reference value f_{20} is thus an

experimental value, not one calculated from the surface tension, density, and drop size, and each data point consists, therefore, of two consecutive measurements of the resonance frequency. The short elapsed time between the two measurements minimizes the uncertainty associated with a change in drop size due to evaporation.

The results are plotted in figure *5* where the relative shift in the resonance frequency f_2/f_{20} is shown as a function of the deformation (a/b). A very slow decrease in the resonance frequency is obtained for initially low oblate deformation, and, within the experimental uncertainty, higher values of a/b (larger deviation from the spherical geometry) always leads to a lowering of the measured resonance frequency. These results are in qualitative agreement with those obtained with laboratory-based levitators, but a close quantitative match was not obtained, except at very large values of a/b. The shift in the resonance frequency measured in 1 g was based on a *calculated* reference value obtained from equation (2) for uncharged drops (Q=0). This is because undistorted levitated drops can only be obtained in 1 g for very small sample radius (R<0.05 cm). Such small size droplets are heavily damped, and a driven resonance frequency is difficult to measure precisely. The current results are also in general agreement with previously obtained 1 g and microgravity data from other investigators 55.

3.2.2 Fundamental Resonance Frequency Variation with Static Electric Field

The shift in the fundamental resonance frequency of ultrasonically driven shape oscillations of levitated drops with an oblate equilibrium shape has been measured as a function of the magnitude of a static (DC) electric field. Both charged and uncharged drops have been investigated. These measurements have been obtained in an Earth-based laboratory, and they are more difficult to interpret because of the influence of both the ultrasonic and electric fields on the drop dynamics. In order to minimize the coupling between these two force fields, we have carried out measurements for very low amplitude acoustically-driven shape oscillation with a *constant* ultrasonic levitation force as a function of the magnitude of the DC electric field, and for increasing surface charge values below the Rayleigh limit. Measurements of the absolute value of the surface charge were not carried out since we were mainly interested in the relative shift in the resonance frequencies of normal modes as a function of both electric field and charge.

The following procedure was adopted for the quantitative. determination of the variation of the driven resonance frequencies: (1) A drop was deployed and levitated ultrasonically, (2) The drop size and shape were measured using its digitized video image, (3) The driven resonance frequency for the axisymmetric fundamental mode (l=2, k=0) and zero electric field was first measured by maximizing the signal from the photodetector, , **(4) The same** measurement was then repeated for at most five increasingly higher static E field values, (5) A final measurement was made for E=O. Each resonance frequency measurement took about 10 seconds, and the whole set of six to seven data points could easily be carried out in less than 90 seconds. The drop size and shape were again measured after each series of measurement to ensure that the drop volume change due to evaporation was small (< 0.5 %) and that the ultrasonic force stayed constant (drop aspect ratio a/b change less than 0.5%). Only the data sets satisfying these conditions were recorded. The relative frequency was plotted as a function of a normalized electric field ($E=E^*(\varepsilon_0 R/\sigma)^{1/2}$). The liquid surface tension σ was measured by a pendant drop technique, and the viscosity was determined by a Cannon-Fenske type apparatus. The drop size ranged between 0.2 and 0.3 cm diameter, and the liquids used were distilled water and a low-viscosity aqueous solution of glycerol (3.25 CP dynamic viscosity).

Figure 6 reproduces a representative data set for uncharged drops and for drops carrying two different charges. The charges Q1 and Q2 have been induced on the drops by imposing voltages of -2 and -3 kV respectively to the electrode connected to the drop injection needle prior to sample deployment and levitation. The. maximum estimated experimental uncertainty in the resonance frequency measurement is 0.5 % (or 0.3 to 0.4 Hz absolute uncertainty). Typical frequencies ranged between 60 and 80 Hz. The continuous curves shown on the graph are third order polynomial least-square fits through two sets of data. The results show a drastic decrease in the driven fundamental resonance frequency for an increasing static electric field intensity. This decrease is even more accentuated by the presence of free surface charge on the drop. “l’his is in qualitative agreement with available analytical and numerical predictions [28,30].

A strict comparison with existing theories is not possible, however, because the shape of the levitated drop does not remain constant as the magnitude of electric field is increased. The initially oblate, ultrasonically levitated drop is deformed by the increasing static field which tends to restore it to a more spherical or even prolate shape. The change in resonance frequent y measured in this particular experi nent thus includes the effects of the

electric field together with the influence of the equilibrium drop shape on the resonant oscillations.

3.3 Nonlinear Characteristics of Driven Large Amplitude Drop Shape oscillations

Three-dimensional *driven* shape oscillation resonant modes have been excited by using levitated millimeter-size low viscosity droplets and modulated ultrasonic radiation pressure or an AC electric field. The equilibrium shape of these ultrasonically levitated drops is oblate with aspect ratio a/b having values between 1.2 and 1.3. The characteristics of the frequency response to these driven excitations are highly sensitive to the drop viscosity: a change from 1.0 to 3.25 CP in the dynamic viscosity brings about a qualitative change in the spectrum of the measured three-din tensional resonant modes for the fundamental l=2 shape oscillations. As we shall describe in the following sections, three separate resonances can be experimentally determined for pure distilled water, and large amplitude driven oscillations lead to a complicated coupling between these three modes. For a higher viscosity liquid (water-glycerol solution with 3.25 CP dynamic viscosity), only two resonances can be observed, and large amplitude driven oscillations can lead to hysteresis and random coupling. The multiplicity of the modes disappears for liquids with viscosity higher than 10 cP , and a single broad peak is obtained.

Fairly large amplitude shape oscillations for the first few shape oscillation modes (l=2,3,4) have been observed when either of the modulation frequency ω_m (see equation 4), or twice the electric field frequency $2\omega_e$ *(see* equation 1) coincides with the appropriate resonance frequency. **Figure 7** shows photographs of instantaneous drop profiles of resonant mode oscillations obtained by using strobed back illumination. The higher mode number resonant oscillations have been experimentally recorded by levitating 4 mm diameter droplets and using substantial modulation of the acoustic radiation force. Although there exists a multiplicity of distinct three-dimensional oscillatory motions for each mode number 1, and corresponding to $k \neq O$, *they* cannot be all experimentally driven with the same ease. In general, for each of the fiist three primary resonances (l=2,3,4), only a subset of all the three-dimensional modes can be excited at moderate oscillation amplitude.

Because the multiplicity of three-dimensional, non-axisymmetric modes quickly increases with higher primary mode number 1, experimental studies of internal mode coupling rapidly become quite complicated. In order to reduce the level of complication, we

have first concentrated on the fundamental resonant mode (l=2) in our discussions of the internal coupling involving three-dimensional modes, of the sub-harmonic mode excitation, and of the hysteresis effect. Energy exchange between resonant oscillations with different primary mode numbers will be discussed in the last section dealing with driven and freely-decaying shape oscillations. All the results described below were obtained with effective drop diameter between 3 and 4 mm, and all the experimental results to be described from this point on have involved electrically *uncharged* drops. All levitated droplets were undergoing randomly oriented residual rotation with a maximum rotational velocity of 1 rps. Through a still unknown mechanism, this residual rotation was substantially reduced, however, as soon as the drops were driven into axisymmetric shape oscillations.

3.3.1. *Non-Axisymmetric Three-Dimensional Resonant Mode Coupling*

Three resonances are experimentally observed for distilled water and *low shape oscillation amplitude:* at the lowest frequency (f^a_2) is a resonance corresponding to vibration with maximum displacement at the poles and very small motion at the equator (oscillations in a vertical plane), the middle resonance (f^b_2) is associated with maximum displacement at the equator and limited motion at the poles (oscillations in a horizontal plane), and finally the highest frequency (f^c_2) resonance corresponds to the usual oblate-prolate mode with the amplitude at the poles being twice at large as at the equator. Figure 8 is a schematic representation of the motion associated with each of these three resonant oscillatory responses. The ratios of the frequencies have the consistently reproducible values of f_{C_2} / f^b_2 = 1.22 and f^c_2 / f^a_2 = 1.4. For low oscillation amplitudes (maximum surface displacement less than 10% of the equilibrium drop diameter), the same results are obtained for both methods of shape oscillation excitation (acoustic force modulation and time-varying electric field).

As the oscillation amplitude is increased by stepping up the acoustical or electrical force excitation, the first resonant oscillations lose axial symmetry and the initially vertical plane vibrations are mixed with running waves resulting in *ordered* three-dimensional motions. These three-dimensional oscillations can be driven in a wide frequency range centered on the initial lowest resonance, and as the frequency is further increased, they are abruptly replaced by the oscillations in a horizontal plane. Increasing the frequency even further excites a mixture of three dimensional modes which can be identified as the pure

(l=2, k=1), (l=2, k=2), (l=2, k=0), modes and a combination of the pure modes. These modes appear to be excited at random, intermittently, and in succession even when the drive frequency and amplitude are kept constant. A second isolated broad resonance can be identified at higher frequency, and corresponds to a large amplitude oblate-prolate oscillation coupled to a running wave.

Figure 9 illustrates the observed drop oscillation geometries for k=0, 1,2 and for the "running wave" mode observed at the higher frequency. The l=2, k=0 mode motion is the usual axisymmetric oblate-prolate oscillation with vertical displacement nearly twice that of the horizontal amplitude (figure 9a). The 1=2, k= 1 mode is a periodic wobble about the vertical axis (Figure 9b), while the l=2, k=2 is an oblate-prolate oscillation about an axis in the plane normal to the vertical axis of symmetry with no displacement along the vertical direction [9] (figure 9c). As shown in the photographs in figure 9, the experimentally observed oscillations are not pure modes, and coupling persists even though the major pure mode characteristics can be easily identified. For example, the l=2, k=2 oscillations observed in figure 9C still display motion along the vertical axis, indicating residual coupling with the 1=2, k=0 mode. In general, coupling of the k=O oscillations with the k=l mode occurs at slightly lower frequency than with the k=2 mode, suggesting that the splitting of the degeneracy by the static shape deformation causes the latter resonance to be at higher frequency, In the presence of a static electric field, the k=O and k=l driven resonances appear at lower frequency, while the k=2 mode *increases* in frequency, in agreement with theoretical predictions (Feng and Beard, 1991 b). The last, "running wave" type of oscillation (figure 9d) cannot be readily classified, but one might speculate that it is a *combination mode* of all three types of oscillations having a well defined and significantly higher resonance frequency.

For a higher viscosity liquid (3.25 cP) only two resonances can be identified. At first approach, the first resonance peak is easily associated with the axisymmetric k=O mode, and the second one (found at higher frequency) is a three-dimensional mode which appears to be a combination of axisymmetric oblate-prolate oscillations and of a surface running wave. Upon closer inspection of the first resonance, however, and upon increasing the shape oscillation amplitude, the three dimensional modes (with k=l and k=2) *can be* individually driven at frequencies very close to that of the axisymmetric mode. A definitive assignment of a resonance frequency to each of the pure. mode cannot be reliably obtained, however, due to the substantial overlap of the three modes within a small frequency range. At large enough oscillation amplitude, periodic energy exchange between the axisymmetric

and non-axisymmetric modes takes place in the same manner as described in the case of the lower viscosity liquid. For very large oscillation amplitude a sudden transition can be induced from seemingly stochastic three-dimensional shape oscillations to *axisymmetric, large amplitude, oblate-prolate oscillations* as the frequency is swept downward *below the first* resonance peak frequency. This *hysteresis* effect is only observed when the electric field drive is used, and it will be further discussed in the next section. For a drive frequency within the *second* resonance, however, the stochastic three-dimensional oscillations never transition to an axisymmetic motion, and the drop is eventually split by the combination of shape oscillations and rotation induced by the running-wave instability. Further, coupling between the large amplitude shape oscillation mode and the resonant translational mode (l= 1) where the restoring force is supplied by the ultrasonic levitation, can lead to sample instability due to vertical oscillations and eventually to a loss of levitation. This coupling can arise due to subharmonic interaction when the shape oscillation frequencies are approximately twice the translational mode resonance frequency.

For liquid with viscosity equal to or greater than approximately 10 cP, only a single broad resonance corresponding to the (l=2, k=0) oscillations can be found. This axisymmetric mode can be maintained to very large oscillation amplitude without coupling to the three-dimensional modes, but it degenerates into a combination of oscillation and running wave when the drive frequency is increased above the broad resonance peak frequency. Viscosity effectively inhibits the energy exchange between the various three-dimensions.1 oscillations characteristic of the fundamental resonant mode and thus enhances the large-amplitude axisymmetric mode stability.

3.2.2 Hysteresis of the Fundamental Mode Response to a Time-Varying Electric Field

The outcome of a sweep of the time-varying electric field frequency across the first resonance of a levitated drop of water-glycerol solution (3,25 cP viscosity) depends on the sweep direction when the *oscillation amplitude becomes large*. When the frequency is increased, the axisymmetric mode is first excited with growing amplitude. As the frequency is further increased and the drop displacement amplitude reaches significant values, the non-axisymmetric resonances are excited, and the. oscillations become three-dimensional with the stochastic and intermittent appearance of pure as well as combination modes. This is described in **figure** 10 where the output of the photodetector monitoring the drop shape is plotted as a function of the electric field frequency. At fixed E-field

amplitude, the E-field frequency was caused to sweep from 55 to 85 Hz, then back from 85 to 55 Hz at 0.25 Hz/sec. The l=2 mode was thus sub-harmonically excited. At these large amplitudes, the resonance curve has leaned so far to the left that it has become triple-valued, with an unstable branch. Such a saddle-node bifurcation has long been recognized as a characteristic feature of nonlinear driven oscillators (Morse and Ingard (1986)"; Parlitz et al. (1992)[61]). This is the first observation of such a phenomenon in a free oscillating drop. What is unique and unexplained, however, is the observation that the crossing of the saddle-node boundary on the downsweep is either preceded or is simultaneous with a shape instability. As the bifurcation frequency is approached from above, and at the maximum prolate phase of the oscillation, a wobbling motion of the drop with respect to the axis of symmetry is observed. After no more than a few cycles of the 1=2 oscillation, the amplitude drop precipitously to the original non-resonant value.

This hysteresis *cannot* be observed with water because coupling to three-dimensional modes prohibits any significant increase in the axisymmetric mode amplitude. Further, hysteresis *cannot* be observed when the *acoustic* force modulation is used to induce shape oscillations in the absence of an electric field. When a *steady* (DC) electric field is present, however, acoustic force modulation will allow the observation of hysteresis. The electric field thus appears to exert a stabilizing action on the large amplitude shape oscillations.

3.3.3. *Soft Nonlinearity in the Resonant Oscillations*

In view of the evidence described in the preceding paragraph, it should not be surprising to find that the resonance frequency of *driven* fundamental mode shape oscillations decreases as the amplitude increases. This has been theoretically predicted [8,9,11,16] and experimentally verified for immiscible liquid systems[14] and falling liquid drops in a gas[15]. Recent results from a Space Shuttle-based experiment carried out in microgravity also support the existence of a soft nonlinearity with quadratic dependence on the oscillation amplitude for *freely decaying* drop shape oscillations[62]. We report here corroborating data for both driven and freely decaying shape oscillations of droplets levitated in air and at 1 G. The shape oscillations have been driven by the time-varying electric field. Although these results are for non-spherical uncharged drops, they are of more practical use to ground-based dynamic methods for surface tension and viscosity measurements using the levitation approach.

Driven oscillation data are more difficult to analyze because of the steady-state drop deformation which is generated together with the time-varying oscillatory motion (Feng and Beard, 1991 a)[28]. Since steady-state drop distortion has also been shown to alter the resonant mode frequencies, observed shifts in these frequencies are the results of the combined effects due to nonlinearity and static shape distortion. In these particular experiments, the ultrasonically levitated droplet already has an oblate equilibrium shape, and the steady-state shape-distorting contribution of the time-varying electric field will tend to drive it into a more spherical shape. The net, experimentally observed effect has been a *consistent lowering of the resonance frequency* of the axisymmetric fundamental mode (l=2, k=0) of shape oscillations for increasing displacement amplitude. Figure 11 describes experimental results obtained for a water-glycerol mixture where the drop oscillatory response recorded by the optical detector has been plotted as a function of the electric field frequency for different field strengths. The frequency shift can be measured through the determination of the change in peak frequency (figure 11a), or by the change in frequency for 90 degrees phase shift at resonance (figure 11 b). Both methods yield similar results (within 2%). The composite plot in figure 11c graphically demonstrates the soft nonlinearity for driven oscillations. The second peak found at the highest electric field drive reflects the excitation of the "running wave" mode previously described.

Quantitatively similar results are obtained when the acoustic force modulation drive is used to excite the shape oscillations. In this case, because the static distortion associated with the oscillatory drop response results in a more *oblate* shape, one can conclude that the contribution from the static deformation is minor compared to the purely nonlinear aspects of the oscillations.

The results depicted in figure 11c have been gathered over a 9 minutes time period. Appreciable drop evaporation takes place over such a time frame, and a correction via normalization has been folded into the analysis of the results. In view of all these experimental complications, we have preferred to rely on the *free-decay* dynamics for frequency shift measurements. In this approach, drop shape oscillations are first driven at an experimentally determined resonance frequency, and the frequency of the free-decay phase after the excitation drive has been terminated. A functional fit to the damped oscillations allows the empirical measurement for the frequency and damping time-constant. The frequency obtained by a fit at the high amplitude portion of the decay trace can be compared to the equivalent measure obtained at the late portion of the decay phase

where low amplitude oscillations take place. Under these conditions, both the effects of static deformation and evaporation can be virtually eliminated, and a large data sample can be acquired over a very short time.

Direct measurements of the time-dependent drop shape have been gathered through the analysis of digitized video images obtained at high frame rate (2,000 frames per second). The backlit drop contours were analyzed using the standard spherical harmonics expansion, and the $c_l(t)$ coefficients (see equation 5) were determined for l=2 to l=6 for *axisymmetric* oscillations. Figure 12 is a sample of the resulting plot for the $c_2(t)$ coefficient obtained from the decay of a 3 mm diameter drop initially driven at resonance. A functional fit involving an exponentially decaying sinusoidal time dependence optimized for the large amplitude portion is shown on the graph, emphasizing the increase in the characteristic decay frequency at low amplitude. A measurement of the oscillation amplitude from the digitized images, and a functional fit at the lower amplitude end provide the necessary information to determine the frequency shift as a function of oscillation amplitude. Such an experimentally determined dependence is displayed in **figure 13** where the percent relative frequency shift $\omega_2(t=\tau)-\omega_2(t=0)/\omega_2(t=\tau)$ (where τ is the experimental elapsed time after which the fit to the low amplitude oscillation is initiated) is plotted as a function of the oscillation amplitude normalized to the equatorial radius of the quiescent levitated oblate drop. Qualitative agreement with previous experimental results in liquid-liquid immiscible systems[14] can be observed, but a quantitative corroboration of the available theoretical predictions cannot be obtained. This is not surprising due to the constraints imposed by both the ultrasonic and electric fields.

3.3.4. *Sub-Harmonic Driven Resonances*

Driven shape oscillation resonances are usually observed when the frequency of the time-varying stimulus coincides with the appropriate resonance frequencies. When the magnitude of the time-varying driving force is high enough, however, a *secondary sub-harmonic resonance* can also be obtained where the driving frequency is *twice* the resonance frequency. In this particular work, we have observed sub-harmonic response when the ultrasonic modulation frequency $\omega_m = 2\,\omega^*$, or when the time-varying electric field frequency $\omega_e = \omega^*$, where ω^* is the frequency of the observed resonance. We report here results for the sub-harmonic excitation of the l=2 and l=3 modes.

When the electric field frequency ω_e has a value nearly equal to the fundamental quadruple mode ω_2, the actual electrically-driven time-varying distortion has a frequency equal to $2\omega_e$ which is close to that of the l=3 resonance mode, ω_3. Under ideal circumstances and when the amplitude of the drive is sufficiently high, both these modes should be excited : the l=2 mode through a secondary and the l=3 mode through a primary resonance. In actual experimental situations, however, the ability to drive asymmetrical modes such as l=3 oscillations depends on both geometrical factors as well as on their damping characteristics. For highly symmetrical levitator configurations, it is not possible to directly excite large amplitude 1=3 oscillations because the subharmonic 1=2 secondary resonance takes precedence. It is possible, however, to induce the three-lobed l= 3 oscillations through the secondary resonance path by setting $\omega_e = \omega_3$.

Figure 14 describes results of experiments on driven and free-decay of sub-harmonically driven fundamental quadruple oscillations using a 3 mm diameter droplet of water-glycerol mixture. The various Legendre coefficients $c_l(t)$ obtained from the digitized video drop images, are plotted on the same scale as functions of time (figure 14a). The calculated volume has also been plotted, and the recorded fluctuations of less than 1 % confirm that the oscillations are essentially axisymmetric. In this particular example ω_e = ω_2 = 439.6 rad/sec (or 70 Hz). Figure 14b displays the FFT of these time-series traces, and shows the drive frequent y peak at 140 Hz and the generated sub-harmonic drop response at 70 Hz. In this case, not only is the l=3 mode directly excited at ω_3, but much higher amplitude 1=2 oscillations also appear at ω_2. The higher order coefficients c_4 (t), $c_5(t)$, and $c_6(t)$, also show non-zero values, but they oscillate mainly at the fundamental frequency ω_2. This is in agreement with the theoretical result from Feng and Beard (1990)[28], predicting that the description of the oscillatory response at each frequency involves several Legendre polynomials.

The sudden decrease of the zero amplitude line in the $c_2(t)$ plot is a manifestation of the steady shape deformation associated with the electrically-driven oscillations. Because a high electric field amplitude is required to drive a sub-harmonic response the drop is statically deformed into a more prolate shape; this is reflected by an increase in the $c_2(t)$ value of the zero amplitude line during the driven oscillations phase. As the AC electric field is shut-off, thus eliminating this static shape deformation, the free-decay phase is initiated and the zero-amplitude line shifts to a more negative C_2 value corresponding to a more oblate equilibrium shape.

3.4 Resonant **Modes Coupling**

We present here experimental results obtained from the analysis of digitized high-speed video images of oscillating drops in both the steady-state driven as well as free-decay modes. In a typical experimental sequence, the drop is first excited into *resonant* oscillations of the appropriate mode number through either direct or sub-harmonic drive. The shape oscillation drive mechanism is then abruptly terminated, and the free-decay phase is recorded with a high-speed video camera at 2,000 frames per second (4,000 fps for higher mode number oscillations such as l=4). Two options are available when shutting off the oscillation drive: the time-varying electric field can be set to zero, or its frequency can be abruptly increased to a high frequency outside of the drop response frequency range (i.e. 500 Hz). The first approach allows the observation of both oscillatory motion as well as of the *steady-state deformation* induced by the time-varying electric field drive. The second option permits the measurement of the free-decay of the oscillatory motion alone as the steady-state deformation is still induced by the higher frequency AC electric field. A corollary situation exists in the case associated with modulated acoustic radiation pressure.

The principal results are :

(1) The profiles associated with each resonant axisymmetric mode driven at a *sing le* frequent y are described by several Legendre coefficients of *different orders,* implying that the dynamic shapes of large amplitude resonant oscillations are characterized by a combination of multiple Legendre shapes.

(2) In general, even-numbered modes do not easily couple to the odd-numbered oscillations, while odd-numbered driven modes can excite even-numbered mode shapes.

(3) Very little energy is transfered to higher modes *(at their respective resonant frequencies),* and this weak mode coupling is significantly hampered by viscous dissipation.

(4) Energy transfer to lower modes and to non-axisymmetric motion is much more prevalent for both driven and free-decaying oscillations.

(5) The free-decay phase of initially oscillating, electrically driven droplets is greatly influenced by the precursor oscillation mode shape and frequency: the characteristic frequency of each Legendre coefficient is dominated by the initial conditions, and the natural modal free oscillations are superposed on the decay of the initial forced oscillations.

Figures 14a and 14b describe an example of a case when the fundamental quadruple resonance is initially driven sub-harmonically (the electric force frequency is twice the drop response frequency, i.e. $\omega_e = \omega_2$). A noticeable. 1=3 response can be measured due to direct excitation at 140 Hz, but a much larger l=4 response is detected at the l=2 mode frequency of 70 Hz. Much smaller contributions from the l=5 and 1=6 components can also be detected, and their primary frequency components are ω_3 and ω_2 respectively. In this particular case, even though the large amplitude oscillations are those of an even-numbered mode, odd-numbered modes are also excited because of the presence of the ω_3 frequency component in the drive mechanism. Very little energy transfer to higher normal modes at their natural frequencies is detected at this oscillation amplitude (about 20% of the equivalent spherical diameter). Even in the free-decay phase, the frequency of oscillation of the higher order coefficients c_4 and c_6 is *the same* as that of the fundamental mode C_2. Only at the end of the free-decay phase can the characteristic frequency $(3\omega_2)$ of the l=4 mode be detected, as shown in figure 1 S where both the time variations of the C_2 and C_4 coefficients are plotted.

The separation of the odd and even-numbered oscillations is even more apparent when the quadruple drop oscillations are directly excited by the time-varying electric field (i.e. ω_e = (1)2/2). This case is illustrated in **figure** 16a and b where both the time-series and FFTs for the first five Legendre coefficients are plotted using the. same scale. The large amplitude 1=2 oscillations generate significant l=4 and l=6 responses at the same frequency of 60 Hz, but l=3 and l=5 oscillations are barely measur able. A more symmetrical shape of the decay curve envelope for the fundamental mode reflects a lower voltage required to drive a primary resonance and consequently a smaller static shape distortion associated with the time-varying electric force. The very asymmetrical oscillations of the higher order Legendre coefficients probably reflect the asymmetry of the electric field drive which is biased towards the elongation of the drop in the vertical direction. The fluctuations in the calculated volume are caused by deviations from axial symmetry due. to probable coupling with three-dimensional resonant modes at large amplitude oscillations. As in the previous case, virtually no evidence of coupling to the higher resonance modes could be obtained, although the FFTs of the l=4 and l=6 coefficients both reveal an unexplained harmonic

component at 120 Hz. Also note that the decay constant is the same for all the Legendre coefficients, strongly suggesting the existence of a single mode.

Fairly large amplitude oscillations of the l=4 resonant modes can be observed when low viscosity liquids such as water are used. Figure 17 presents the time series of the Legendre coefficients of a levitated water drop initially driven in the third resonant shape mode. In this case both higher and lower mode number synchronous oscillations are detected in the driven phase. Because relatively high electric field intensities are required to drive the higher, more damped modes, a substantial static shape distortion accompanies the time-dependent shape oscillations. Definite coupling to the fundamental mode in the free-decay phase is revealed by the time variations of the C_2 coefficient where a lower frequency component immediately appears upon termination of the electric field drive. These results can be compared with Basaran's predictions[16] based on the numerical simulation of the decay process of a drop initially distorted in a *static* shape based on a Legendre coefficient c4=0.3 for a liquid drop with a Reynolds number Re=100 ($Re=1/\nu(\sigma R/\rho)^{1/2}$). The experimental findings are for Re=360, the drop is initially oscillating, and the decay trace envelope is asymmetrical. The essential features, however, are consistent with the numerical simulation results except that the l=4 frequency component is absent from the theoretically derived time variations of the l=6 and higher coefficients. Experimental results also show noticeable 1=3 and l=5 components synchronous with the l=4 driven oscillations.

A similar experiment was also performed in low gravity during a Space Shuttle flight by one the authors (EHT). A *rotating* drop of water was acoustically positioned in air, and modulation of the acoustic radiation pressure was used to drive it into steady-state l=4 resonant shape oscillations prior to observing a free-decay phase obtained by turning off the amplitude modulation of the positioning sound field. The video-recorded sequence has been analyzed, and the results are presented in figure **18.** The space-based data show negligible contribution from the odd-numbered coefficients, and confirm the coupling to the lower frequency fundamental mode. The dominance of the fundamental natural mode, however, is immediate upon initiation of the free-decay phase. Synchronous oscillations of the c_2 and c_6 coefficients similar to the ground-based results are also obtained. The modulation of the fundamental mode oscillations (observed in the c_2 and volume plots) is caused by the onset of three-dimensional modes as the constraining amplitude modulation of the sound field is turned off. **Figure 19** presents results for a drop in low gravity oscillating about an oblate shape and driven by modulated acoustic radiation pressure.

These results have been obtained from 16 mm cinefilm records which are more dificult to digitally analyze, but they are very similar to those presented in **figure 17** for a droplet levitated on the ground and driven into oscillations by a time-varying electric field.

4. DISCUSSION AND SUMMARY

The principal objective of this experimental investigation was to carry out specific quantitative observations of the dynamic response of free drops levitated in the Earth gravitational field. The motivation was to study the nonlinear aspects of these motions within the framework of an already substantial body of analytical and numerical predictions, but also to better assess the influence of ultrasonic and electric fields on these phenomena in order to effectively exploit the capabilities of single fluid particle levitation techniques for various Earth-based as well as low-gravity applications. In view of the evidence uncovered thus far, we are comforted by the fact that theoretical predictions have been shown to be consistent with most of our findings when the experimental conditions closely approximate the theoretical constraints. On the other hand, we have also determined that both acoustic radiation pressure and electric field stresses and free charges significantly modify the dynamic response of free drops. Although a general theoretical framework for the analysis of the isolated static effects of acoustic and electric fields exists, a detailed analytical or numerical study of all the relevant factors influencing the behavior of a levitated drop in 1 g is not yet available.

Measurements of the static deformation of levitated drops under the combined action of acoustic radiation and electric field stresses have been carried out for the first time as a first application of the hybrid levitation technique. The opposite actions of the acoustic (oblate-biased) and electric (prolate-biased) forces have been shown to allow the continuous controlled shaping of the drop. No theory combining both field effects is currently available.

The static oblate deformation associated with ultrasonic levitation of liquid drops has been determined to induce a decrease in the resonance frequency of driven quadruple small amplitude shape oscillations. This fact had already been established by prior experimental studies for substantially deformed levitated drops in 1 g[54], but recent low gravity measurements have confirmed this decrease for slightly deformed droplets. 'I'his has a significant impact on those ground-based methods of surface tension measurement

relying on the determination of the resonance frequency of oscillating drops. In the presence of a static electric field, this frequency has also been shown to significantly decrease, even for spherical drops. The presence of a net surface free charge was also shown to accentuate the lowering of the frequency. The experimental results we have described in this paper, however, concern ultrasonically levitated charged and uncharged droplets under the influence of a static electric field. Although the outcome of this study is in qualitative agreement with available theoretical predictions, a detailed analysis of the results requires the assessment of the effects of both the static oblate deformation as well as of the ultrasonic restoring force.

The decoupling of the non-axisymmetric quadruple modes from the usual oblate-prolate axisymmetric oscillations has been experimentally verified for oblate ultrasonically levitated drops. Three isolated resonances with characteristic oscillatory motions can be identified for low viscosity liquids, but increasing the viscosity gradually results in the eventual merging of these peaks into a broader resonance curve. The presence of a static electric field shifts the resonance frequency of two of the modes downwards (l=2, k=0 and 1=2, k=1), but the last mode (l=2, k=2) frequency is rai seal, as predicted by a theory based on asymptotic expansion[28] , At large oscillation amplitude, coupling, between these closely spaced modes takes place and this generally leads to seemingly three-dimensional and temporally complex oscillations. Under the excitation due to a time-varying electric field hysteresis can be observed for the oblate-prolate mode which is driven to very large amplitude before a surface instability abruptly and dramatically decreases the high amplitude driven response. This hysteresis effect cannot be observed when the drop oscillations are excited by modulated acoustic radiation pressure, although in this case, the presence of a *static* electric field will bring it back.

Sub-harmonic excitation of shape oscillation triodes has been observed when the frequency of the time-varying stimulus is twice the relevant resonance frequency. This secondary resonance phenomenon has also been theoretically predicted[28] , and it allows the indirect excitation of resonant modes not driven through the standard primary resonance. For example, asymmetric, odd-numbered resonant modes such as the l=3 oscillations can only be driven to substantial amplitude through the secondary resonance route.

Even at fairly large amplitude shape oscillations, very little energy is transferred from lower-order modes to higher-order resonances. When axisymmetric shape oscillations are decomposed into their linear components represented by the Legendre

polynomials, driven resonant oscillations at a single frequency are described by several time-varying Legendre coefficients. Even in the free-decay region, the time dependence of the first few Legendre coefficients is dominated by the driven oscillations. When a higher-order mode is driven and subsequently turned off, coupling to lower order modes can be observed at their natural frequency, suggesting that viscous dissipation is the primary influence in the mode coupling process, Microgravity experimental results obtained with droplets positioned in air by acoustic radiation force are very similar to the ground-based data, suggesting that high intensity ultrasonic and electric fields modify the observed drop dynamics quantitatively, but not qualitatively.

ACKNOWLEDGMENTS

This work was performed in collaboration with Professor L.G. Leal of the Chemical and Nuclear Engineering department at the University of California at Santa Barbara, and it was carried out at the Jet Propulsion Laboratory, California Institute of Technology under contract with the Microgravity and Life Science Division of the National Aeronautics and Space Administration.

REFERENCES

1. Kaji, N., Mori, Y. H., and Tochitani, Y., "Heat transfer enhancement due to electrically induced resonant oscillations of drops", ASME J. Heat Transfer 107,788-793 (1985)

2. Scott, T.C. and Wham, R.M. ,"An electrically driven multistage countercurrent solvent extraction device: the emulsion phase contractor", I. & E. C. Research 28,94-101 (1989)

3. Raina, G. K., Wanchoo, R. K., and Grover, P. D., "Direct contact heat transfer with change of phase: motion of evaporating droplet", AICHE J. 11, 835-837 (1984)

4. Trinh, E. H., Marston, P. L., and Robey, J. L., "Acoustic measurement of the surface tension of levitated drops", J. Colloid Interface Sci. 124,95-103 (1988)

5. Suryanarayana, P. V. R., and Bayazitoglu, Y.," Effect of static deformation and external forces on the oscillations of levitated drops", Phys. Fluids A 3,967-977 (1991)

6. Cummings, D. L., Blackburn, D.A., "Oscillations of magnetically levitated aspherical droplets", J. Fluid Mech. 224,395-416 (1991)

7. *a.* Prosperetti, A.," Normal mode analysis for the oscillations of a viscous drop immersed in another liquid", J. Méc. 19, 149-182 (1980), and *b.* Prosperetti, A.,''Free oscillations of drops and bubbles: the initial value problem", J. Fluid Mech. 100, 333-347 (1980)

8. Foote, G. B., "A numerical method for studying liquid drop behavior: simple oscillations", J. Comput. Phys. 11,507-530 (1973)

9. Tsamopoulos, J.A. and Brown, R. A., "Nonlinear oscillations of inviscid drops and bubbles", J. Fluid Mech. 127,519-537 (1983)

10. *a*. Natarajan R. and Brown R. A., "Quadratic resonance in the three-dimensional oscillations of inviscid drops with surface tension", Phys. Fluids 29, 2788-2797 (1986) and *b.* Natarajan, R. and Brown, R.A., "Third order resonance effects and the nonlinear stability of drop oscillations", J. Fluid Mech. 183,95-121 (1987)

11. Lundgren, T.S. and Mansour, N. N.,''Oscillations of drops in *zero* gravity with weak viscous effects", J. Fluid Mech. 194, 479-510 (1988)

12. Patzek, T. W., Benner, R.E.Jr, Basaran, O.A. and Scriven, L. E.,''Nonlinear oscillations of inviscid free drops", J. Comput. Phys. 97,489-515 (1991)

13. Basaran,O.A., Scott, T. C., and Byers, C. H., " Drop oscillations in liquid-liquid systems", AICHE Journal 35, 1263-1270 (1989)

14. Trinh, E. and Wang T. G., "Large amplitude free and driven drop shape oscillations: experimental observations", J, Fluid Mech. 122,315-338 (1982)

15. Becker, E., Hiller, W. J., and Kowalewski, T. A.,''Experimental and theoretical investigation of large-amplitude oscillations of liquid droplets", J. Fluid Mech. 231, 189-210 (1991)

16. Basaran, O. A., " Nonlinear oscillations of viscous liquid drops", J. Fluid Mech. 241, 169-198 (1992)

17. Becker, E., Hiller, W. J., and Kowalewski, T.A., "Nonlinear dynamics of viscous droplets", J. Fluid Mech. 258, 191-216 (1994)

18. Trinh, E. H., Thiessen, D. B., and Holt, R. G., "Driven and freely-decaying nonlinear shape oscillations of drops and bubbles immersed in liquids", Presented for publication (1995)

19. Taylor, G. I., "Disintegration of water drops in an electric field", Proc. R. Sot. Lond. A280, 383-397 (1964)

20. Brazier-Smith, P. R., 13rook, M., Latharn, J., Saunders, C.P., and Smith, M. H., "The vibration of electrified water drops", Proc. R. Sot. Lend. A322, 523-534 (1971)

21. Miksis, M., "Shape of a drop in an electric field", Physics of Fluids 24, 1967-1972 (1981)

22. Adomato, P.M. and Brown, R.A.,''Shape and stability of electrostatically levitated drops", Proc. Roy. Sot. Lend. A389, 101-117 (1983)

23. *a.* Basaran, O.A. and Scriven, L. E.,"Axisymmetric shape and stability of isolated charged drops", Phys. Fluids A 1, 795-798 (1989), *b.* Basaran, O.A. and Striven, L. E., "Axisymmetric shape and stability of charged drops in an electric field", Phys. Fluids A 1, 799-809 (1989)

24. Pelekasis, N.A. ,Tsamopoulos, J, A., and Manolis, G.D., "Equilibrium shape and stability of charged and conducting drops", Phys. Fluids A 2, 1328-1340(1990)

25. Tsamopoulos, J.A. and Brown, R. A., "Resonant oscillations of inviscid charged drops", J. Fluid Mech. 147,373-395 (1984)

26. Tsamopoulos, J. A., Akylas, T.R. and Brown, R. A., "Dynamics of charged drop break-up", Proc. Roy. Sot, Lend. A 401,67-88 (1985)

27. Natarajan, R. and Brown, R. A., "The role of three-dimensional shape in the break-up of charged drops", Proc. Roy. Sot. Lend. A 410,209-227 (1987)

28. *a.* Feng, J.Q. and Beard, K. V., "Small amplitude oscillations of electrostatically levitated drops", Proc. Roy. SW. Lend. A 430, 133-150 (1990); *b.* Feng, J.Q. and Beard, K. V., "Resonance of a conducting drop in an alternating electric field", J. Fluid Mech. 222, 417-435 (1991a); c. Feng, J.Q. and Beard, K.V.," Three-dimensional oscillation characteristics of electrostatically deformed drops", J. Fluid Mech. 227,429-447 (199 lb)

29. Kang, 1. S., "Dynamics of a conducting drop in a time-periodic electric field", J. Fluid Mech. 257,229-264 (1993)

30. Feng, Z.C. and Leal, L. G., "Numerical simulation of the dynamics of an electrostatically levitated drop", presented for publication (1995)

31. *a.* Trinh, E.H.," Compact acoustic levitation device for studies in fluid dynamics and material science in the laboratory and microgravity", Rev. Sci. Instrum. 56, 2059-2065 (1985), b. Trinh, E.H. and Leung E., "Ground-based studies of the vibrational and

rotational dynamics of acoustically levitated drops and shells", American Institute of Aeronautics and Astronautics, Washington DC, paper 90-0315, (1990)

32. Marston, P.L. and Trinh, E. H., "Hyperbolic umbilic diffraction catastrophe and rainbow scattering from spheroidal drops", Nature 312, 529-531 (1984)

33. Lierke, E. G., Luhmann, D., and Leung, E.," Terrestrial levitation, deformation, and disintegration (atomization) of liquids and melts in a one-axial acoustic standing wave", American Institute of Physics (New York, 1988), Conference Proceedings 197, 71-80 (1988)

34. Tian, Y., Holt, R. G., and Apfel, R. E., "Deformation and location of an acoustically levitated drop", J. Acoust. Sot. Am. 93,3096 (1993)

35. Lee, C. P., Anilkumar, A. V., and Wang, T.G.," Static shape and instability of an acoustically levitated liquid drop", Phys. Fluids A 3, 2497-2515 (1991)

36. Wyatt, P.J. and Phillips, D.T.," A new instrument for the study of individual aerosol particles", J. Coil. Interface Sci. 39, 125-135 (1972)

37. Tang, I.N. and Munkelwitz, H. R., "An investigation of solute nucleation in levitated solution droplets", J. Colloid Interface Sci. 98,430-438 (1984)

38. Rhim, W. K., Chung, S. K., Trinh, E. H., and Elleman, D.D.," Charged drop dynamics experiment using an electrostatic-acoustic hybrid system", Mat. Res. Sot. Symp. Pmt. vol. 87,329-337 (1987)

39. Rayleigh, Lord,"On the equilibrium of liquid conducting masses charged with electricity", Phil. Mag.14, 184- 186(1882)

40. Landau. L.D. and Lifshitz, E. M., *Fluid Mechanics*, Pergamon Press, Addison Wesley, Reading, MA, p, 239 (1959)

41. Marston, P. L., Lo Porto Arione, S.E. , and Pullen, G. L., "Quadruple projection of the radiation pressure on a compressible sphere", J. Acoust. Sot. Am. 69, 1499-1501 (1981)

42. Jackson, H.W., Barmatz, M, and Shipley, C.," Equilibrium shape and location of a liquid drop acoustically positioned in a resonant rectangular chamber", J. Acoust. SOC. Am. 84, 1845-1857, (1988)

43. Tnnh, E.H. and Hsu, C.J., "Equilibrium shape of acoustically levitated drops", J. Acoust. Sot. Am. 79, 1335-1338 (1986)

44. Anilkumar, A. V., Lee, C.P., and Wang, T. G.,"Stability of an acoustically flattened drop: An experimental study", Phys. Fluids A 5,2763-2774 (1993)

45. Taylor, G. I.,''Studies in electrohydrodynamics. I. The circulation produced in a drop in an electric field ", Proc. Roy. Sot. Lend. A 291, 159-166 (1966)

46. Vizika, O. and Saville, D. A., "The Electrohydrodynamic deformation of drops suspended in liquids in steady and oscillatory electric fields", J. Fluid Mech. 239, 1-21 (1992)

47. OKonski, C.T. and Thatcher,H.C., "The distortion of aerosol droplets in an electric field", J. Phys. Chem. 57,955 (1953)

48. O'Konski, C.T. and Harris, F.E., "Electric free energy and the deformation of droplets in electrically conducting systems", J. Phys. Chem. 61, 1172 (1957)

49, Sample, S. B., Ragupathi, B., and Hendricks, C. D.,''Quiescent distortion and resonant oscillations of a liquid drop in an electric field", Int. J. Enging. Sci. 8,97-109 (1970)

50. Pruppacher, H. R., Rasmussen, R., Walcek, C., and Wang, P. K.,"A wind tunnel investigation of the shape of uncharged raindrops in the presence of an external, vertical electric field", *Proceedings of the Second International Colloquium on Drops and Bubbles*, Monterey, 1981, JPL/NASA Publication 82-7, 239-246(1982)

51. Coquillat, S and Chauzy, S., "Behavior of precipitating water drops under the influence of electrical and aerodynamic forces", J. Geophys. Res. 98, 10,319-10,329 (1993)

52. Marston, P.L., "Shape oscillation and static deformation of drops and bubbles driven by modulated radiation stresses-Theory ", J. Acoust. Sot. Am. 67, 15-26 (1980)

53. Trinh, E., Zwern, A., and Wang, T. G., "An experimental study of small amplitude drop oscillations in immiscible liquid systems ", J. Fluid Mech. 115,453-474 (1982)

54. Biswas, A., Leung, E., Trinh, E. H., "Rotation of ultrasonically levitated glycerol drops", J. Acoust. SW. Am. 90, 1502-1507 (1991)

55. Apfel, R. E., Holt, R.G., Tian, Y., Shi, T., and Zheng, X.," Surface characterization through shape oscillations of drops in microgravity and 1-g ", *Joint Launch+ One year Science Review of USML-1 and USMP-1 with the Microgravity Measurement Group,* NASA Conference Publication 3272, volume I, N. Ramachandran, D.O. Frazier, S.L.Lehoczky, and C.R. Baugher Eds., 339-357 (1994)

56. Annamalai, P., Trinh. E.H., and Wang, T. G., "Experimental study of the oscillations of a rotating drop", J. Fluid Mech. 158, 317-327 (1985)

57. Busse, F., " Oscillations of a rotating liquid drop ", J. Fluid Mech. 142, 1-8 (1984)

58. Trinh, E.H. and Robey, J.L, "Experimental study of streaming flows associated with ultrasonic levitators ", Phys. Fluids 6,3567-3579 (1994)

59. JSC Reduced Gravity Program User's Guide, Lyndon B. Johnson Space Center Technical Memorandum JSC-22803, Houston, TX, National Aeronautics and Space Administration, December 1987

60. Morse, P.M. and Ingard, K. U., *Theoretics/ Acoustics,* Princeton University Press (princeton, 1986) pp. 828-855

61. Parlitz, U., Englisch V., Scheffczyk, C. and Lauterborn W., "Bifurcation structure of bubble oscillators", J. Acoust. Sot. Am. 88, 1061-1077 (1990)

62. Wang, T. G., Anilkumar, A. V., Lee, C. P., "Oscillations of liquid drops: Results from the US ML- 1 experiments in space", J. Fluid Mech. at press

FIGURE CAPTIONS

Figure 1.
Schematic description of the experimental apparatus. A drop is shown freely suspended between the driver and reflector of a single axis ultrasonic levitator. A high voltage amplifier driven by a low frequency (DC to 1 kHz) function generator is connected to the reflector, and generates the DC and AC high voltages. The drop motion is recorded by a ccd video camera connected to a recorder and to a microprocessor with a real-time 30 fps frame grabber. For high frame rate application, the ccd camera is replaced by a Kodak Spin Physics high speed camera and recording system. The drop shape can also be monitored by projecting the shadow of the levitated back-illuminated drop onto a photo-detector. The output of this photo-detector is amplified and fed into a digital oscilloscope and spectrum analyzer.

Figure 2.
Photographs of a sequence of shapes captured using strobed illumination. The drop is undergoing large amplitude driven quadruple (l=2, k=0) shape oscillations. Typical fundamental mode oscillation frequencies range between 50 and 100 Hz for the sizes and liquids used in this study.

Figure 3.
Plots of the measured aspect ratio a/b of a levitated water-glycerol drop as a function of the value of the static electric field and for three different fixed sound pressure levels. The drop profile is initially oblate in the absence of any electric field due to the ultrasonic radiation stresses. The action of a DC (static) electric field is to reduce the drop aspect ratio, i.e. to force the drop shape into a more spherical shape. For the acoustic levels used in this example, even high electric field strength up to breakdown value did not force the drop back into an ideal spherical geometry (a/b=1.0).

Figure 4.
Photographs of a sequence of static drop shapes for a fixed ultrasonic pressure and increasing DC electric field strength (from 1 to 10 kV/cm). For a large enough drop, prolate shapes can be obtained within the allowable electric field strength. A noticeable asymmetry can be observed at the high end of the electric field values.

Figure 5.

Plot of the results of measurements of the shift in the driven quadruple ($l=2, k=0$) resonance frequency as a function of the drop static oblate distortion (expressed by the aspect ratio ah). These results were obtained during short-duration periods of low gravity, and they are strictly relative measurements. Each data point corresponds to two consecutive measurements: one at a/b near 1.0 and another one at a relevant higher value of the aspect ratio.

Figure 6.

Plot of the results of measurements of the shift in the driven quadruple resonance frequency as a function of the normalized DC electric field strength for both charged and uncharged drops. The continuous curve through the data points are third-order polynomial fits. For a given DC field strength, a higher free surface charge results in a greater decrease in the resonant frequency.

Figure 7.

Photographs obtained under strobed illumination of the first three driven resonant modes of shape oscillations of an ultrasonically levitated drop. These large amplitude oscillations have been obtained for water droplets using ultrasonic radiation pressure modulation.

Figure 8.

Schematic description of the distribution of the three-dimensional decoupled fundamental resonant modes. For low viscosity liquids such as water three distinct resonances can be identified with characteristic oscillations. For higher viscosity liquids ($\eta > 3$ cP), only two main resonances can be located. The first resonance is broad and contains the three modes which can be individually excited with careful tuning. The second resonance is an oblate-prolate oscillation superposed on a running wave.

Figure 9.

Photographs of single video frames recorded at 30 fps showing the morphologies of the various three-dimensional $l=2$ oscillation modes. a : Axisymmetric l=2, k=0 oscillations; b: l=2, k=l oscillations, c: l=2, k=2 oscillations; d: oblate-prolate and running wave mode.

Figure 10.

Plot of the photo-detector response as a function of the time-varying electric field frequency exhibiting hysteresis. The sub-harmonic response at f of the l=2 mode was monitored with a lock-in amplifier. During the frequency upsweep, the response amplitude suddenly increases at 66-67 Hz. During the downsweep, the amplitude continues to increase until it abruptly drops at about 57 Hz, where it attains the original value. This sudden decrease is preceded by the onset of shape instability.

Figure 11.

Plots of the photo-detector responses as functions of the time-varying E Field frequency for different E field magnitudes. The 1=2 mode response at 2f was measured with a lock-in amplifier. (a): Drop oscillation amplitude for two different E field values. The shift in the maxima gives a measure of the resonance frequency shift. (b) Phase of the drop oscillation with respect to the driving E-field as a function of the E-field frequency at two different E-field values. The resonance frequency shift is measured where the curves cross the 90° line. (c) Same as (a) for five E-field values. The second peak at E=6.05 kV/cm is due to the excitation of the running wave mode at large oscillation amplitude.

Figure 12.

Plot of the time dependent $C_2(t)$ Legendre coefficient obtained from the analysis of digitized high-speed video recordings of the free-decay phase of a 3mm diameter water-glycerol drop. The continuous line is a fit of the data using an exponentially decaying sinusoidal time dependence optimized for frequency match at large amplitude oscillations. The shift in the resonance frequency is clearly demonstrated by the increasing mismatch between the fit and the data at low amplitude oscillations.

Figure 13.

Plot of the free-decay relative frequency shift for the fundamental axisymmetric quadruple mode as a function of the normalized amplitude. The relative frequency shift is obtained by using the ratio of the frequency measured at the last two cycles to the frequency measured at the first two cycles. The normalized amplitude is talc ulated by comparing the maximum vertical amplitude (in the prolate shape) at first cycle with respect to the equilibrium static shape of the levitated drop.

Figure 14.

Plots of the time dependence and FFTs of the first five Legendre coefficients during steady-state drive and free-decay phases of a sub-harmonically excited water-glycerol drop by a time-varying electric field. (a) Amplitude of the Legendre coefficients as a function of time. (b) FFTs of the first five Legendre coefficients. In this particular case, the electric force oscillates at 140 Hz and the largest amplitude drop oscillatory response is at 70 Hz. The l=3 mode is also driven directly at 140 Hz at smaller amplitude because it is more highly damped and because of the slight mismatch between its resonance frequency and the electric field drive frequency.

Figure 15.

Superposed plots of the calculated time dependence of the Legendre coefficients c_2 (t) and C_4(t) at the low amplitude end of the free-decay phase of an oscillating 3 mm diameter water droplet. As the amplitude of the entrained oscillations due to the fundamental mode C_2(t) decreases, higher frequency components are more apparent. In particular, a component near triple the fundamental mode frequency begins to be more clearly defined with decreasing fundamental mode amplitude.

Figure 16.

Time dependence (a) and FFTs (b) of the first five Legendre coefficients of a water-glycerol drop excited into primary resonant oscillations. In this case the electric force oscillates at 60 Hz, and the largest amplitude oscillatory response of the quadruple mode is at 60 Hz. No odd-numbered oscillations are excited to a significant extent. The decay trace envelope for C_2(t) is more symmetrical (compared with that in figure 14a) due to a lesser static drop distortion. The frequency component at 120 Hz for the higher even numbered Legendre coefficients cannot yet be explained.

Figure 17.

Time dependence of the first five Legendre coefficients for a water droplet in the driven and free-decay phases. The initial oscillations are in the l=4 mode, and are directly excited into primary resonance by an electric force oscillating at 143.2 Hz. Fairly large amplitude synchronous oscillations are detected for both l=2 and l=6 shapes, as well as a noticeable l=3 component. The natural resonant oscillations of the 1=2 mode appear at the end of the decay phase.

Figure 18.

Time dependence of a first five Legendre coefficients for a rotating water drop acoustically positioned in microgravity. The l=4 mode oscillations are initially excited by modulation of the acoustic radiation pressure, and the free-decay phase is initiated by turning off the amplitude modulation. The equilibrium shape of the drop is slightly oblate (c_2= -O. 15) due to rotation and acoustic radiation stresses. The odd-numbered coefficients response is negligible, and in contrast with the ground-based results, the dominance of the natural frequency of the fundamental mode (l=2) is immediate upon the termination of the l=4 mode drive.

Figure 19.

Results of the analysis of the driven and free-decay phases of a rotating drop in microgravity and initially driven into the l=4 mode oscillations by acoustic radiation pressure modulation. The data were obtained from 16 mm cinefilm records exposed at 400 frames/second. The noisier quality of the data stems from the non-ideal lighting characteristics which create spurious reflections and highlights on the drop images. These results are very similar to those obtained with droplets levitated on Earth, except for the earlier appearance of the fundamental natural mode at the onset of free-decay.

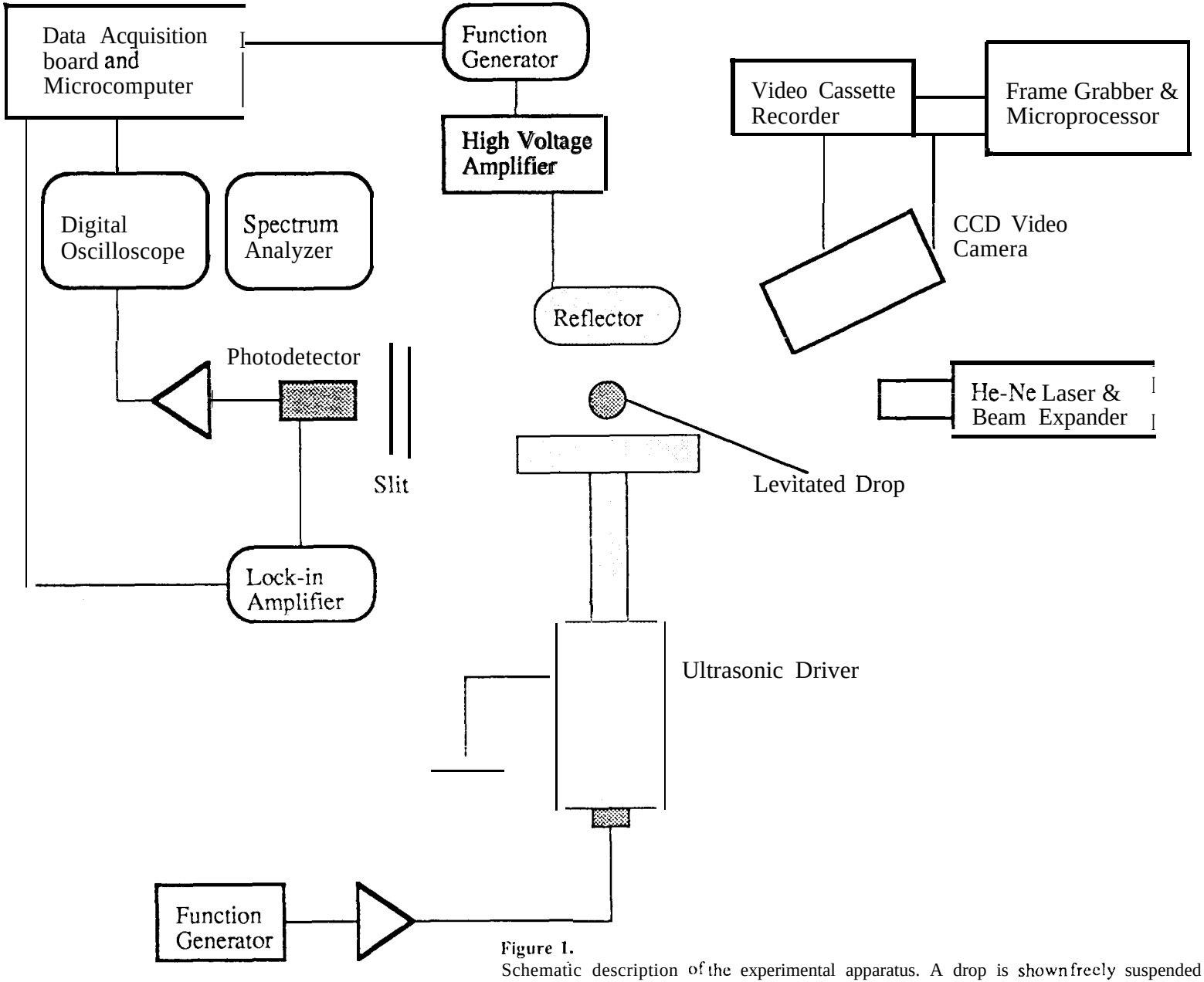

Figure 1.
Schematic description of the experimental apparatus. A drop is shown freely suspended between the driver and reflector of a single axis ultrasonic levitator. A high voltage amplifier driven by a low frequency (DC to 1 kHz) function generator is connected [0 the reflector, and generates the DC and AC high voltages. The drop motion is recorded by a ccd video camera connected to a recorder and to a microprocessor with a real-time 30 fps frame grabber. For high frame rate application, the ccd camera is replaced by a Kodak Spin Physics high speed camera and recording system. The drop shape can also be monitored by projecting the shadow of the levitated back-illuminated drop onto a pholo-detector. The output of this photo-detector is amplified and fed into a digital oscilloscope and spectrum analyzer.

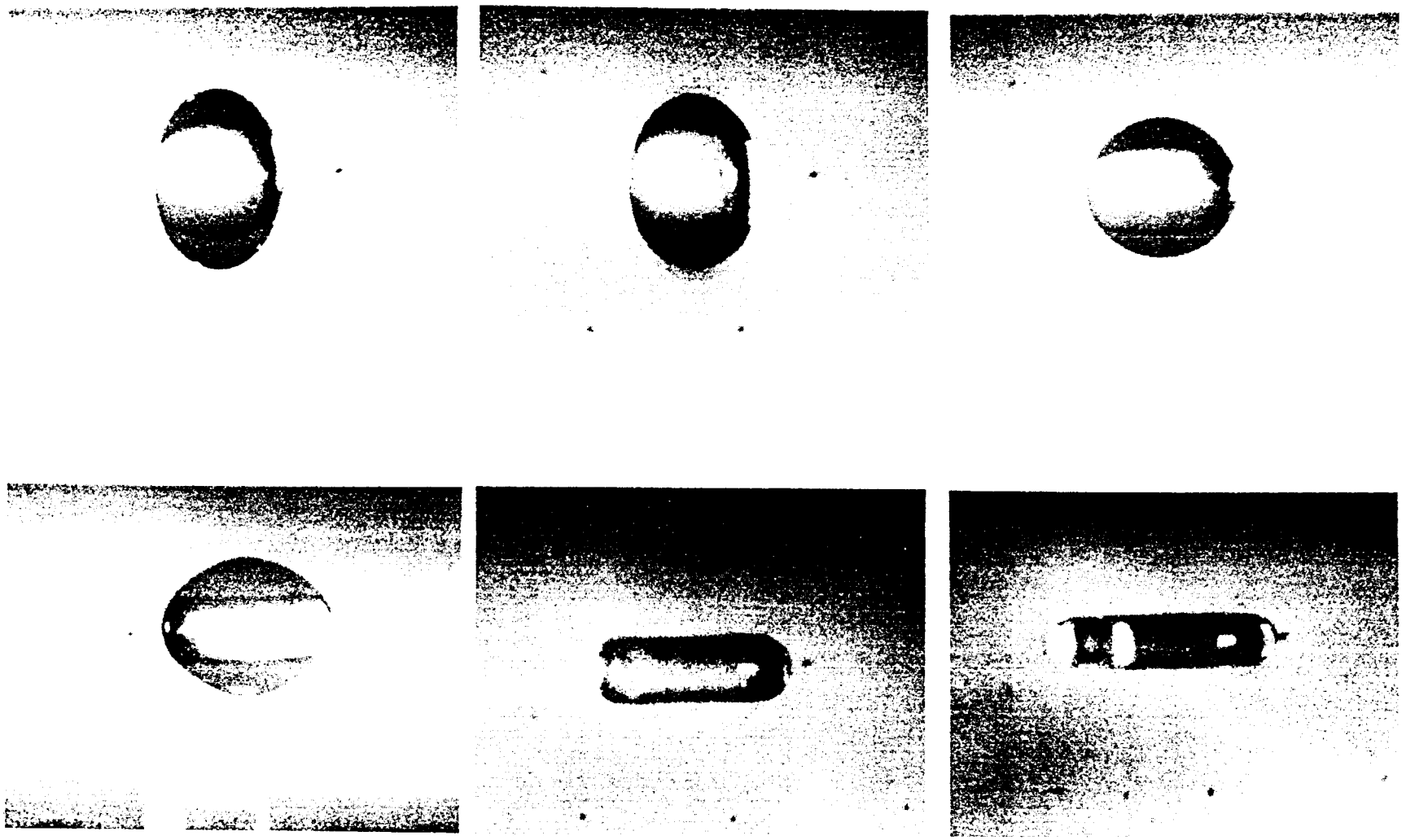

Figure 2.
Photographs of a sequence of shapes captured using strobed illumination. The drop is undergoing large amplitude driven quadrupole (l=2, k=0) shape oscillations. Typical fundamental mode oscillation frequencies range between 50 and 100 Hz for the sizes and liquids used in this study.

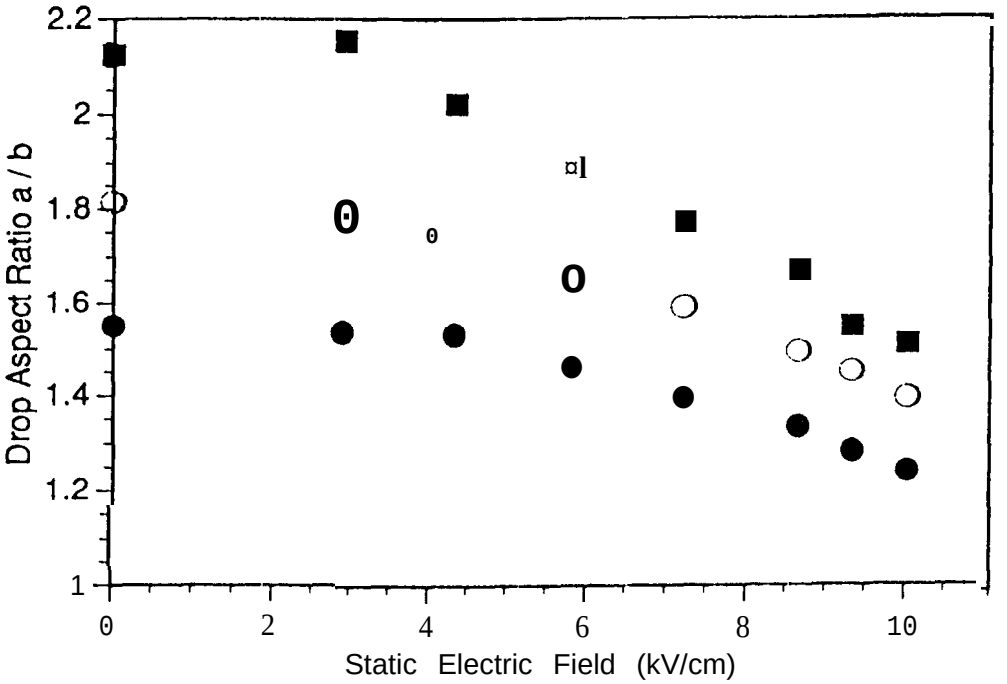

Figure 3.
Plots of the measured aspect ratio a/b of a levitated water-glycerol drop as a function of [hc value of [he static electric field and for three different fixed sound pressure levels. The drop profile is initially oblate in the absence of any electric field due [o the ultrasonic radiation stresses. The action of a DC (static) electric field is [o reduce the drop aspect ratio, i.e. 10 force the drop shape into a more spherical shape. For the acoustic levels used in [his example, even high electric field strength up to breakdown value did not force the drop back into an ideal spherical geometry (a/b=1.0).

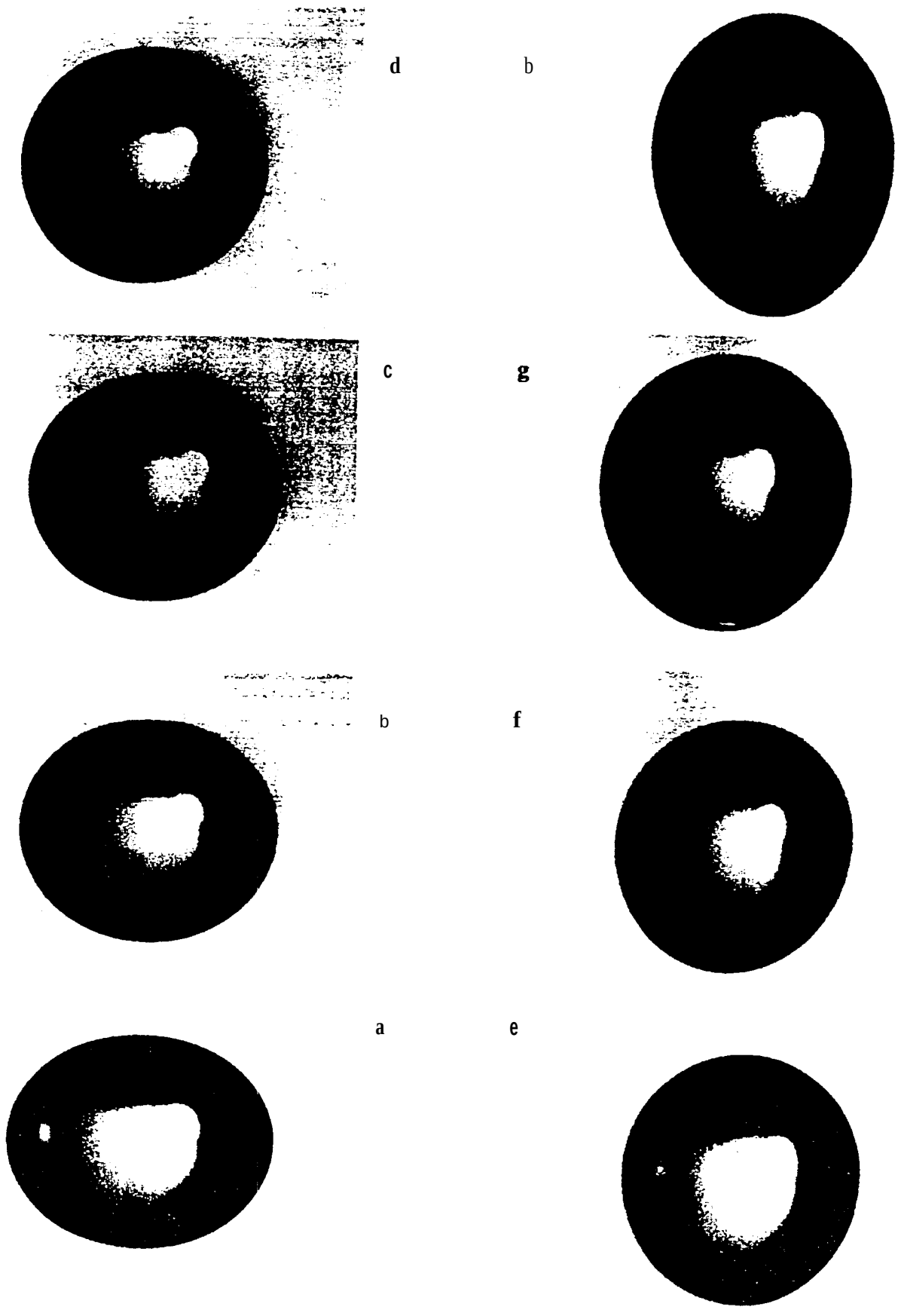

Figure 4.
I'holographs of a sequence of static drop shapes for a fixed ultrasonic pressure and increasing DC electric field strength (from 1 to 10 kV/cm). For a large enough drop, prolate shapes can be obtained within the allowable electric field strength. A noticeable asymmetry can be observed at [hc high end of the electric field values.

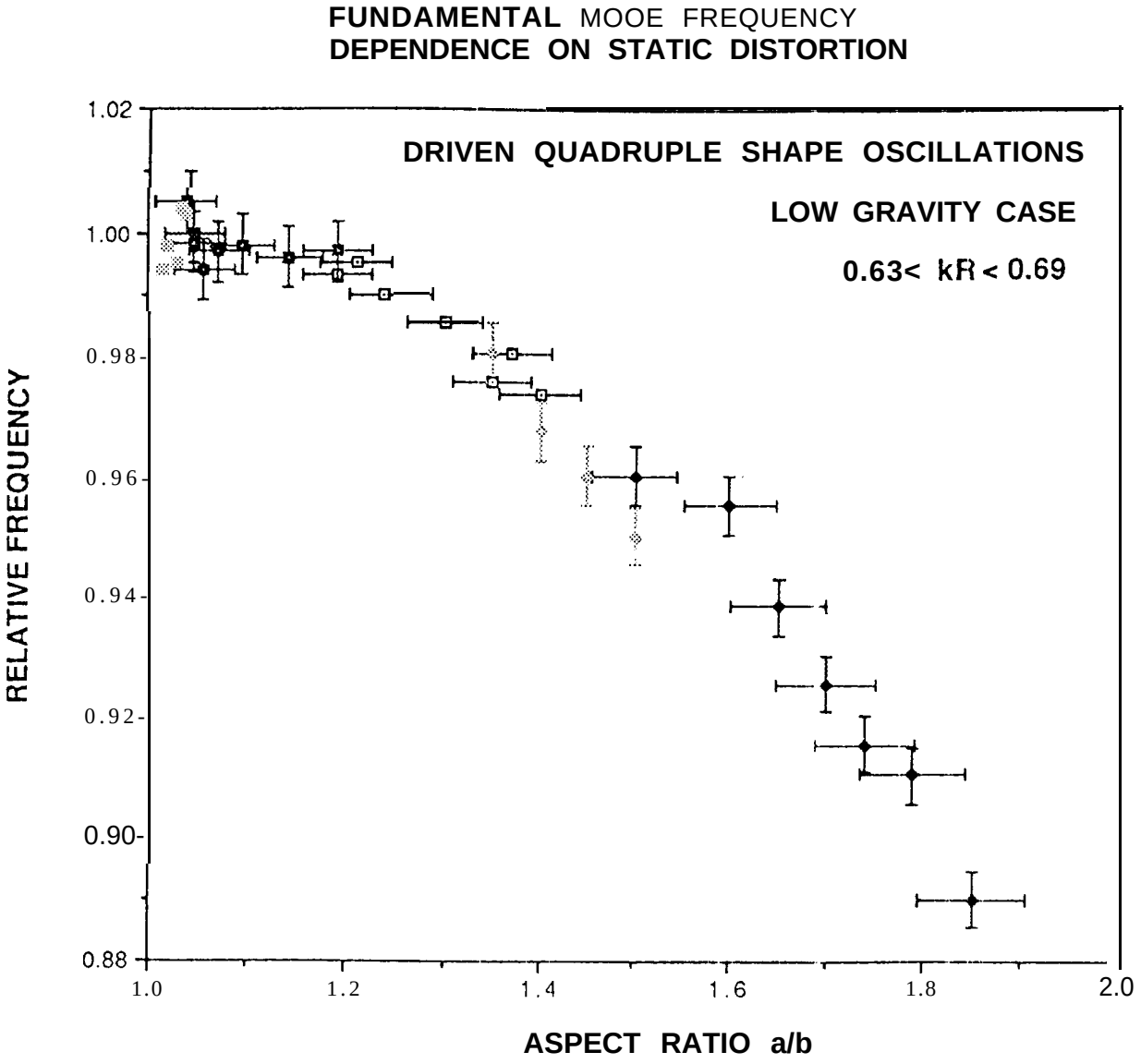

Figure 5.
Plot of the results of measurements of the shift in the driven quadrupole (l=2, k=0) resonance frequency as a function of the drop static oblate distortion (expressed by [he aspect ratio a/b). These results were obtained during short-duration periods of low gravity, and [hey are strictly relative measurements. Each data point corresponds to two consecutive measurements: onc at a/b near 1.0 and another one at a relevant higher value of the aspect ratio,

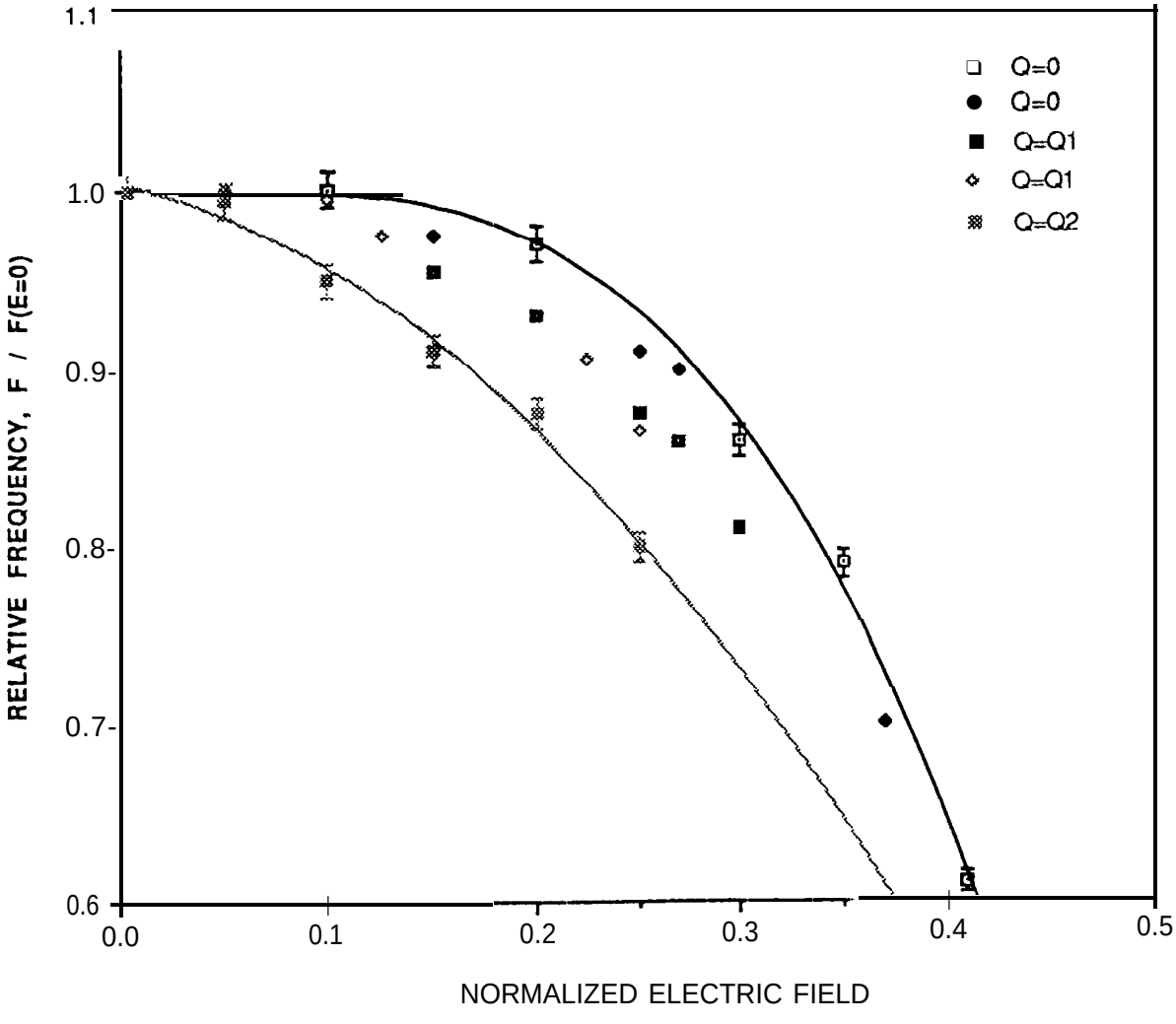

Figure 6.
Plot of the results of measure.nlcnts of the shift in the driven quadrupole resonance frequency as a function of the normalized DC electric field strength for both charged and uncharged drops. The continuous curve through the data points are lhird-order polynomial fits. For a given DC field strength, a higher free surface charge results in a greater decrease in the resonant frequency.

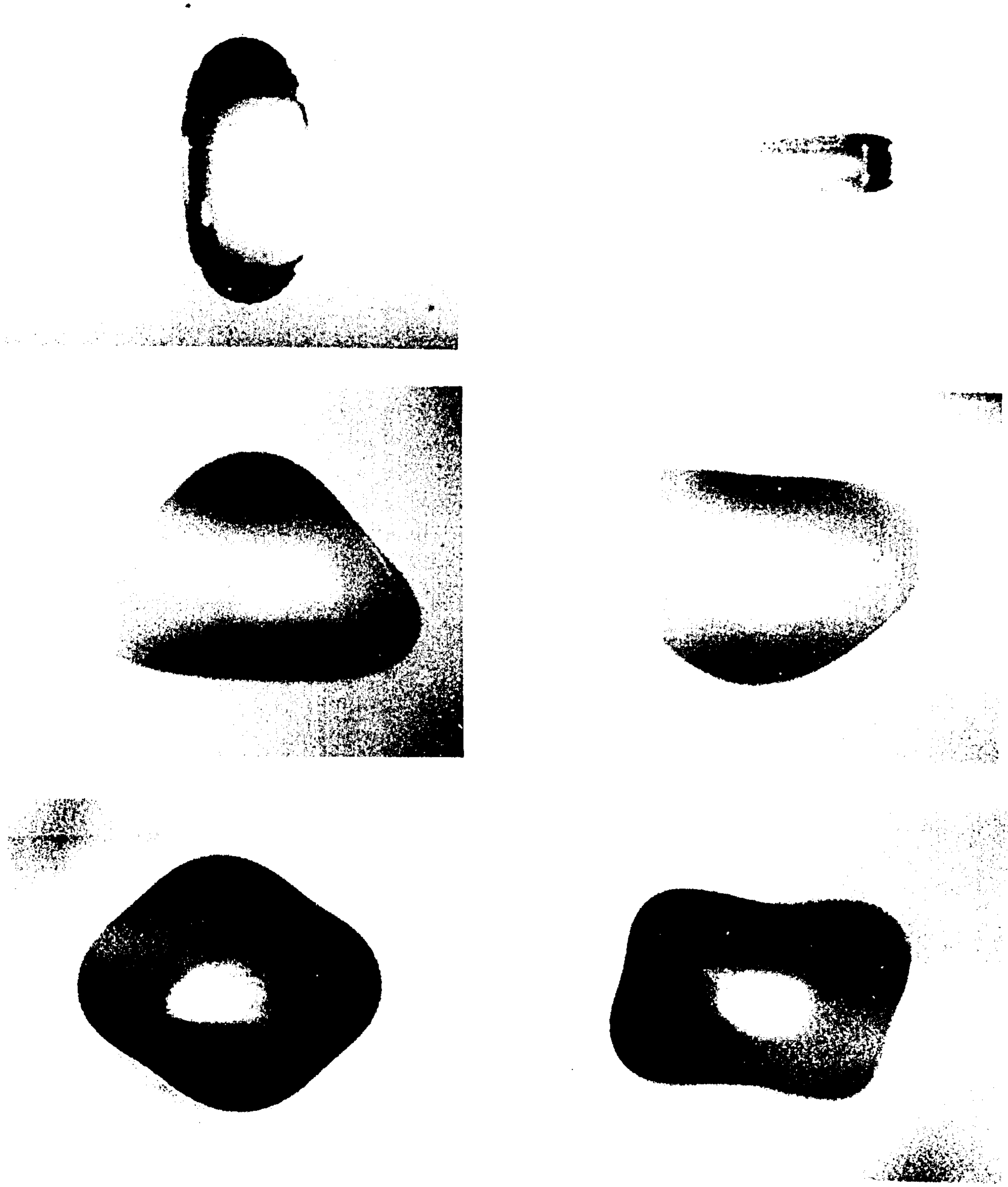

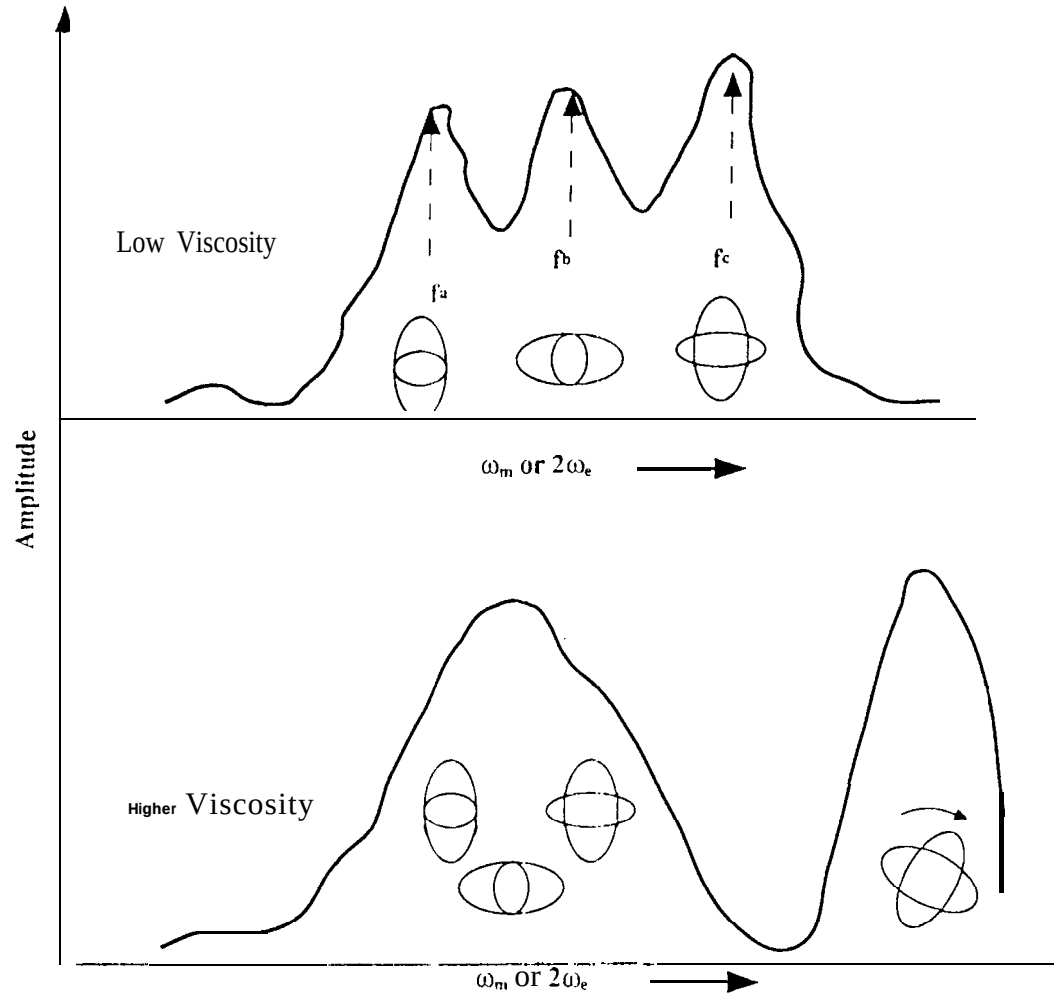

Figure 8.
Schematic description of [he distribution of the three-dimensional decoupled fundamental resonant modes. For low viscosity liquids such as water three distinct resonances can be identified with characteristic oscillations, For higher viscosity liquids ($\eta > 3$ cP), only two main resonances can be located. The first resonance is broad and contains the three modes which can be individually excited with careful tuning The second resonance is an oblatc-prolate oscillation superposed on a running wave,

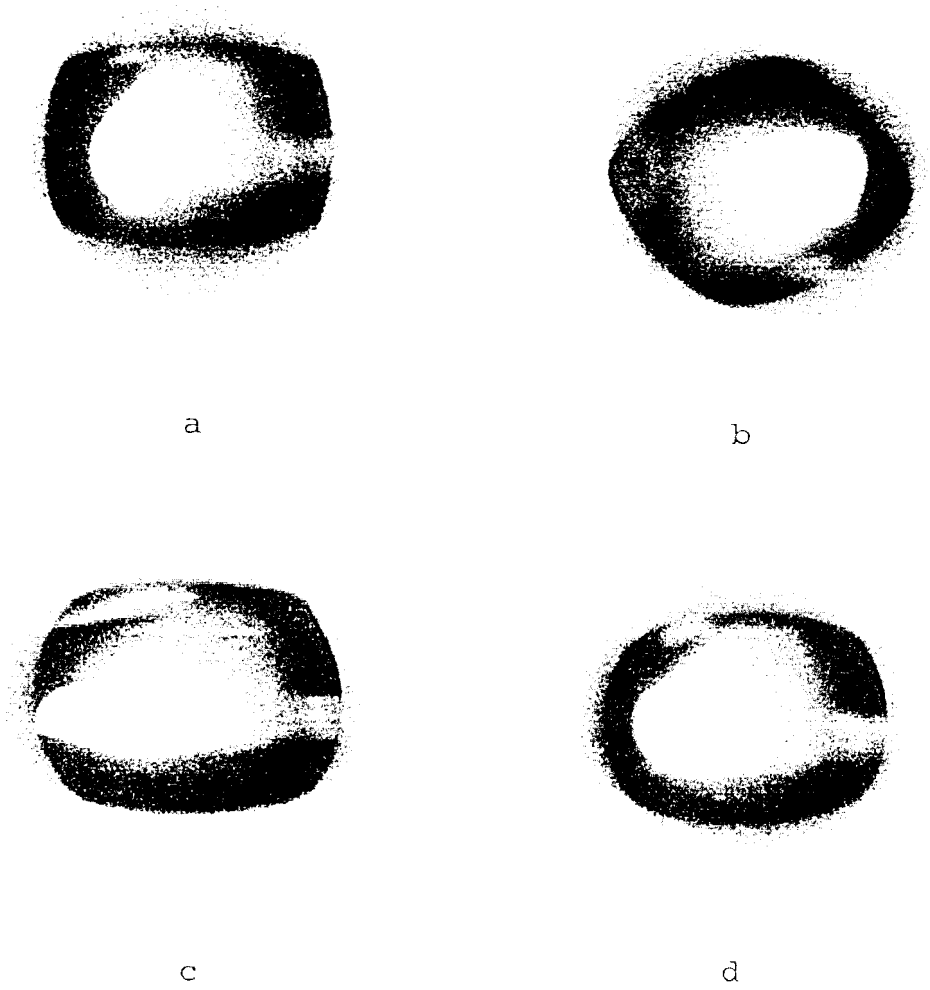

Figure 9.
Photographs of single video frames recorded at 30 fps showing the morphologies of the various three-dimensional l=2 oscillation modes. a : Axisymmetric l=2, k=0 oscillations; b: l=2, k=1 oscillations, c: l=2, k=2 oscillations; d: oblate-prolate and running wave mode.

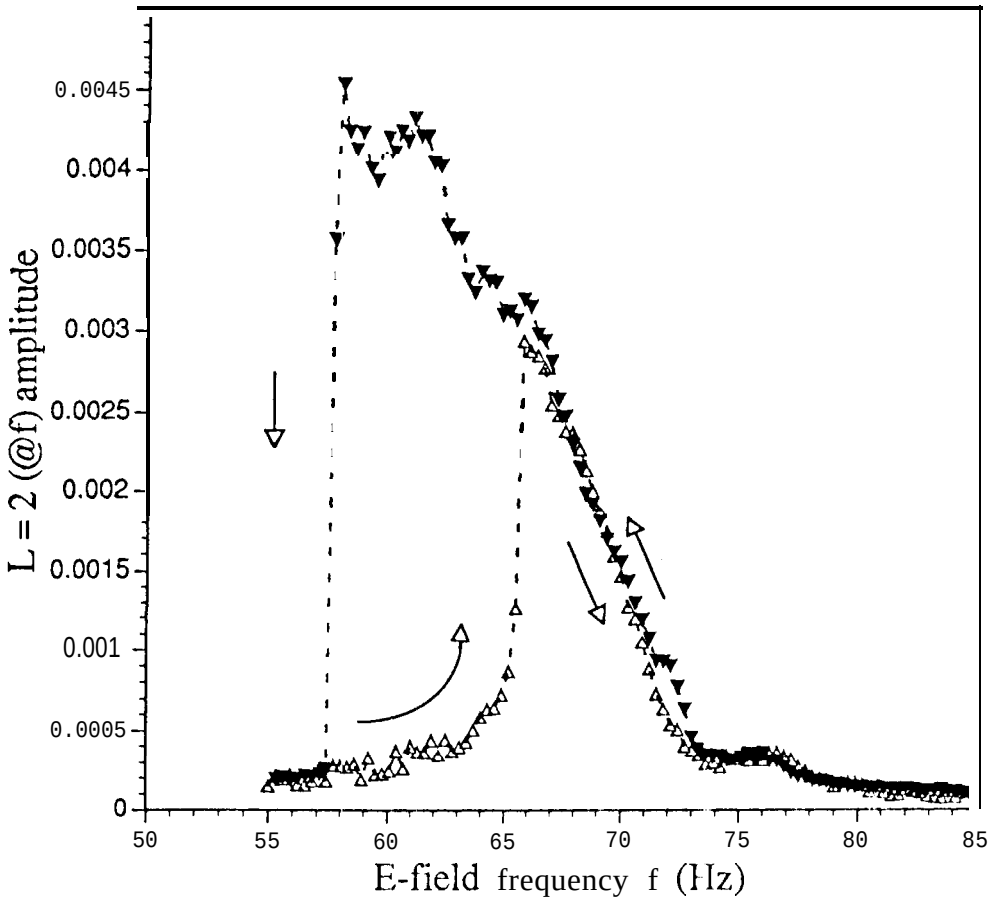

Figure 10.
Plot of the photo-detector response as a function of the time-varying electric field frequency exhibiting hysteresis, The sub-harmonic response at f of the l=2 mode was monitored with a lock-in amplifier. During the frequency upsweep, the response amplitude suddenly increases at 66-67 Hz. During the downsweep, the amplitude continues to increase until it abruptly drops at about 57 Hz, where it attains the original value. This sudden decrease is preceded by the onset of shape instability.

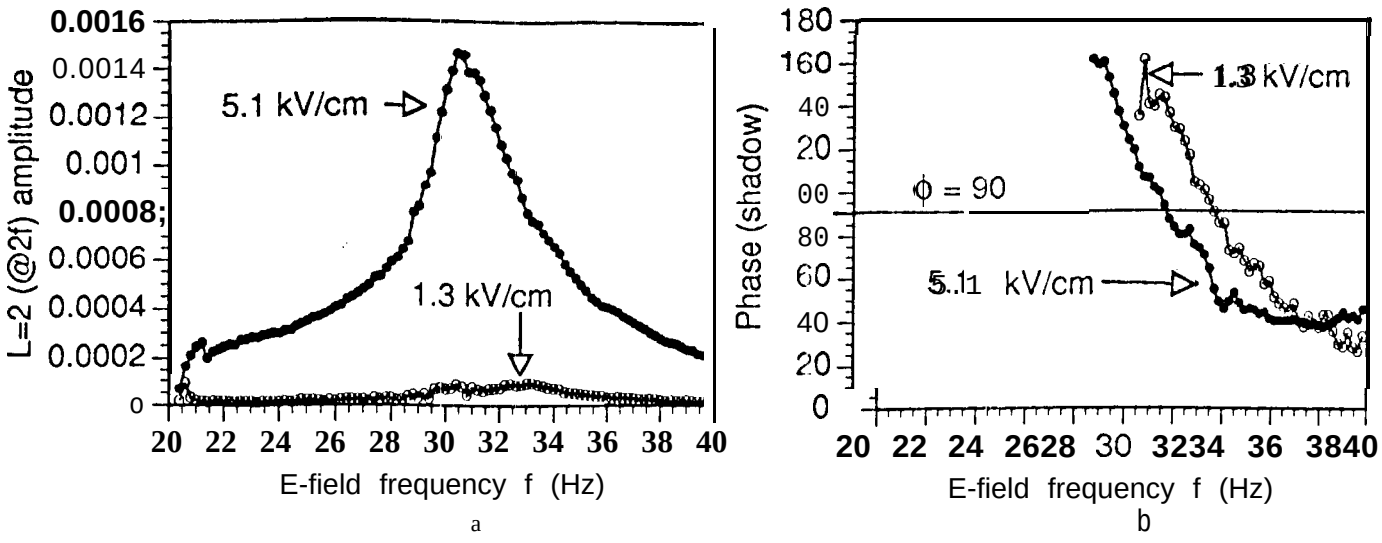

Figure 11.
Plots of the photo-detector responses as functions of the time-varying E Field frequency for different E field magnitudes. The 1=2 mode response at 2f was measured with a lock-in amplifier. (a): Drop oscillation amplitude for two different E field values. The shift in the maxima gives a measure of the resonance frequency shift. (b) Phase of the drop oscillation with respect to the driving E-field as a function of the E-field frequency at two different E-field values. The resonance frequency shift is measured where the curve: cross the 90° line. (c) Same as (a) for five E-field values. The second peak at E=6.05 kV/cm is due to the excitation of the running wave mode at large oscillation amplitude.

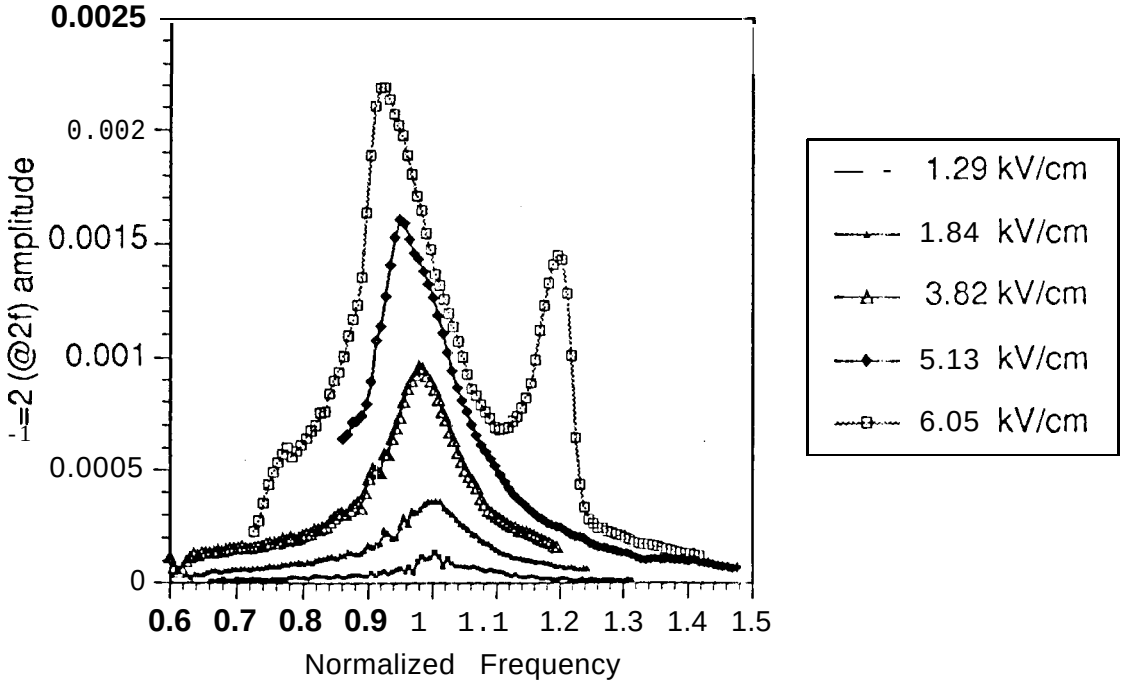

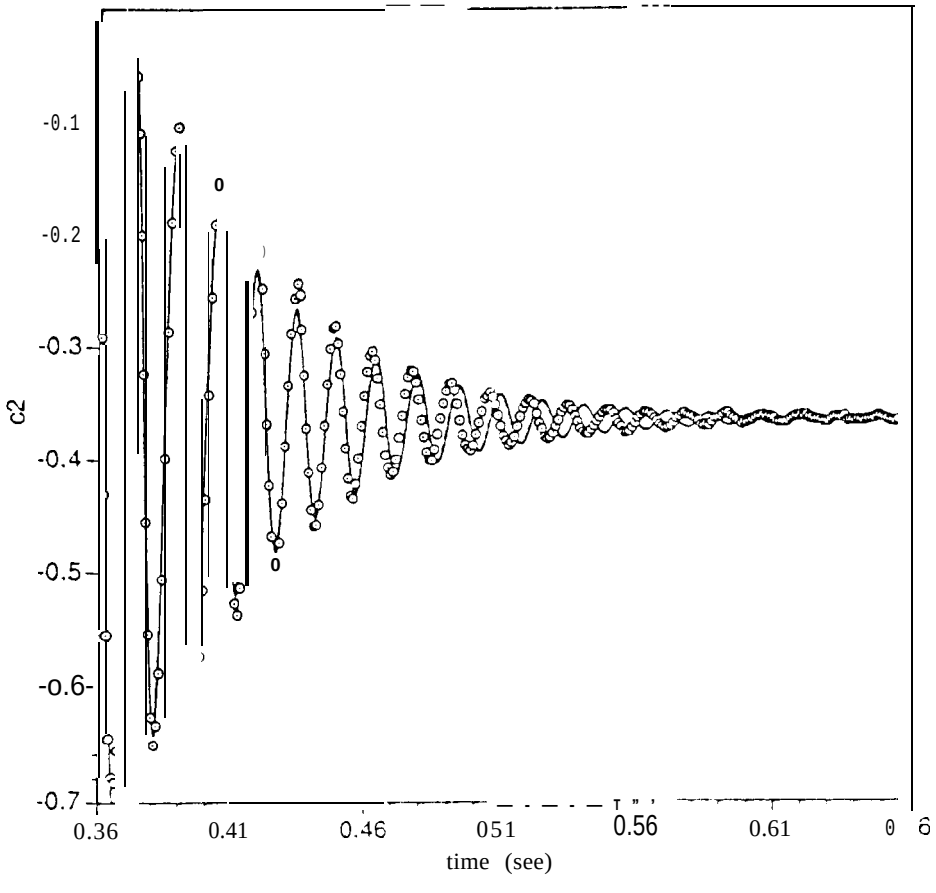

Figure 12.
Plot of the time dependent c2 ([) Legendre coefficient obtained from the analysis of digitized high-speed video recordings of the free-decay phase of a 3mm diameter water-glycerol drop. The continuous line is a fit of the data using an exponentially decaying sinusoidal time dependence optimized for frequency match at large amplitude oscillations. The shift in the resonance frequency at large amplitude is clearly demonstrated by the increasing mismatch between the fit and the dots at low amplitude oscillations.

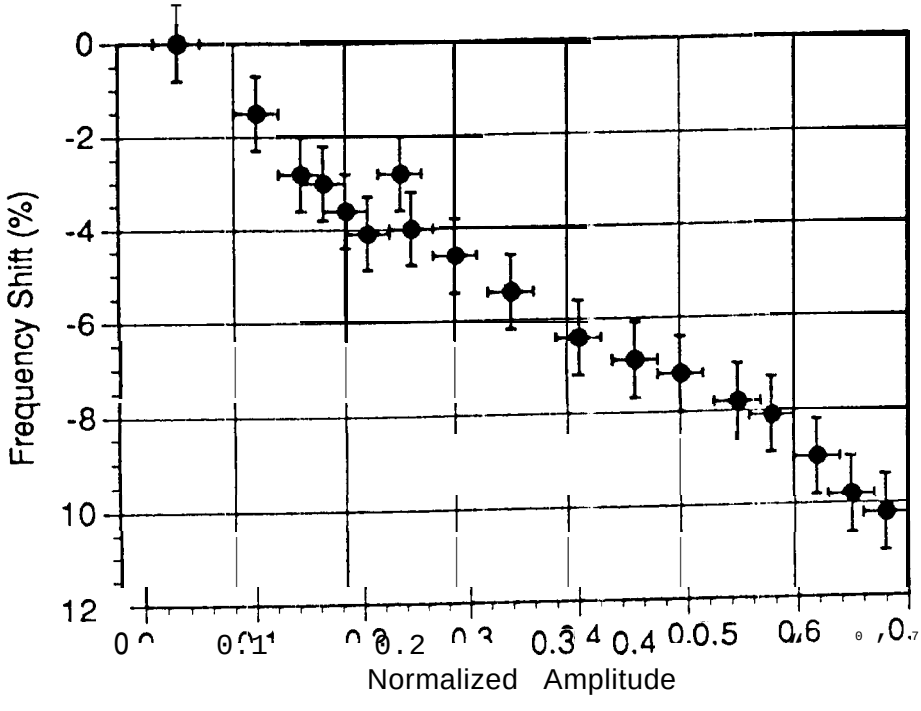

Figure 13.
Plot of the free-decay relative frequency shift for the fundamental axisymmetric quadrupole mode as a function of the normalized amplitude. The relative frequency shift is obtained by using the ratio of the frequency measured at the last two cycles to the frequency measured at the first two cycles. The normalized amplitude is calculated by comparing the maximum vertical amplitude (in the prolate shape) at first cycle with respect to the equilibrium static shape of the levitated drop.

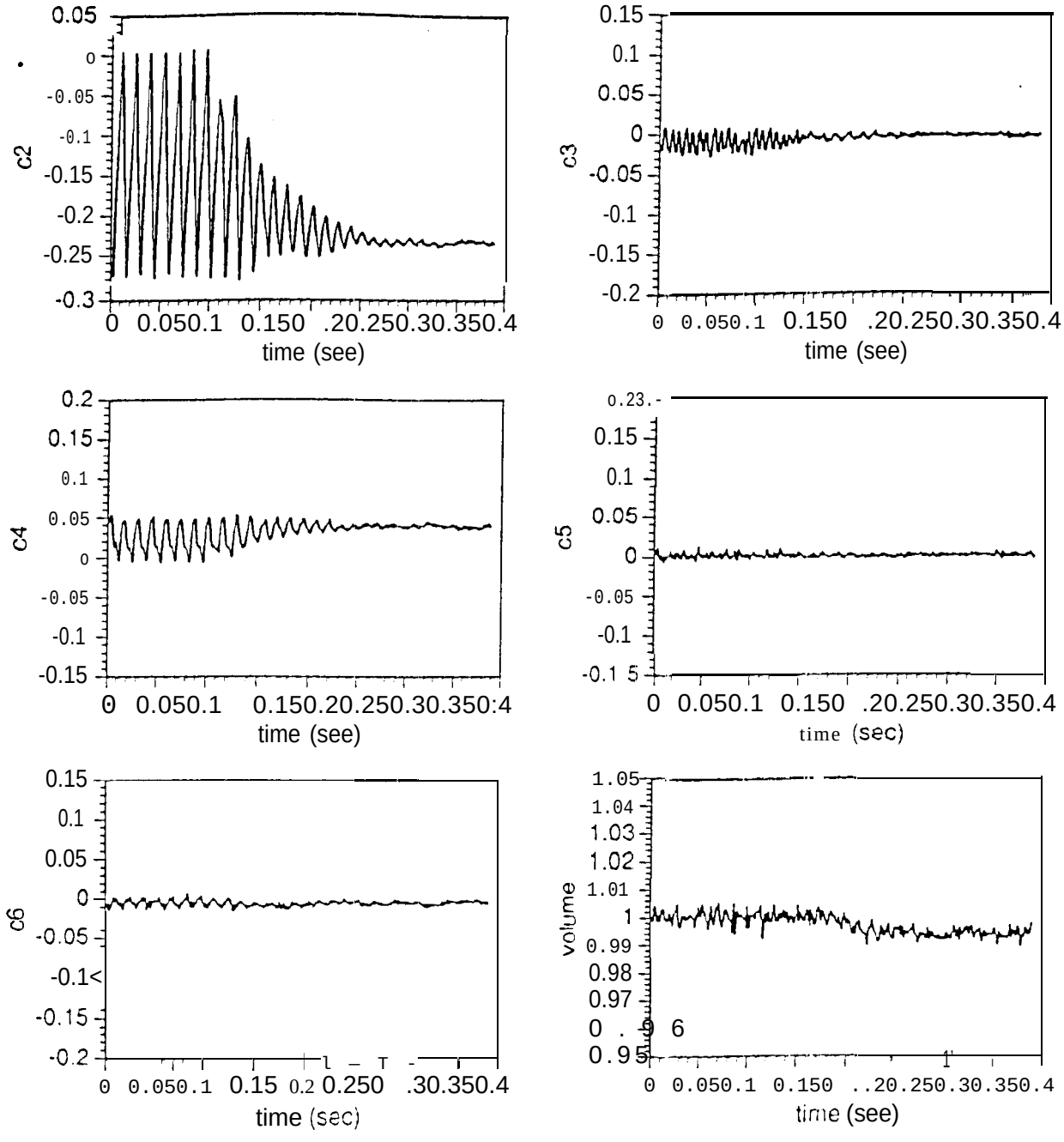

a

Figure 14.
Plots of the time dependence and FFTs of the first five Legendre coefficients during steady-state drive and free-decay phases of a sub-harmonically excited wa[cr-glycerol drop by a time-varying electric field. (a) Amplitude of the Legendre coefficients as a function of time. (b) FFTs of the first five Leg end re coefficients. In [his particular case, the electric force oscillates at 140 Hz and the largest amplitude drop oscillatory response is at 70 Hz. The l=3 mode is also driven directly at 140 Hz at smaller amplitude because it is more highly damped and because of the slight mismatch between its resonance frequency anti the electric field drive frequency.

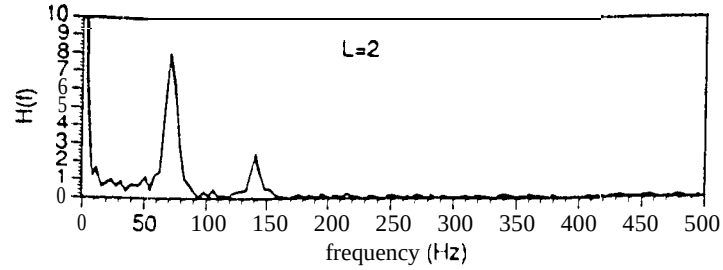
L=2
H(f)
frequency (Hz)

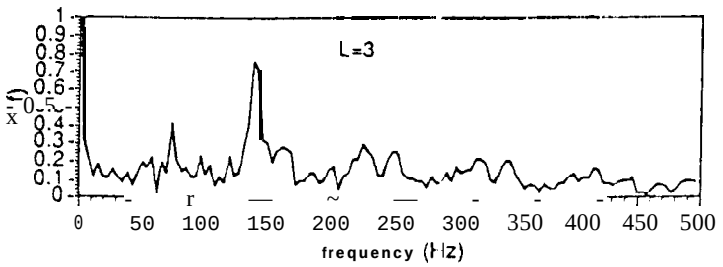
L=3
H(f)
frequency (Hz)

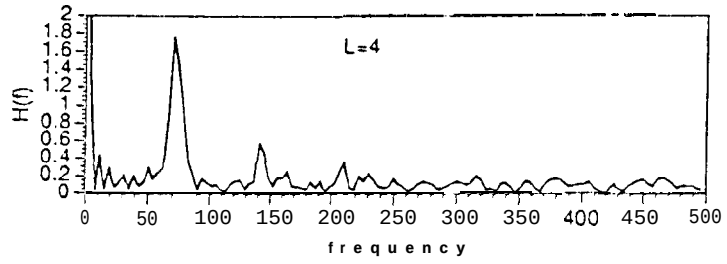
L=4
H(f)
frequency

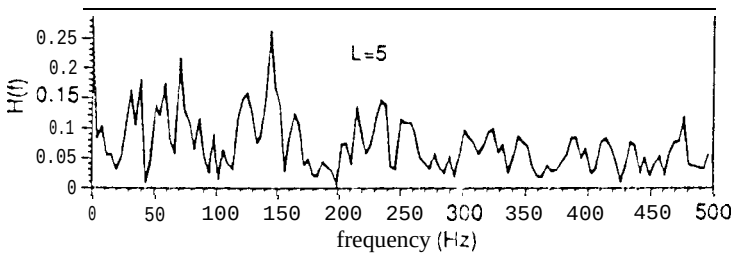
L=5
H(f)
frequency (Hz)

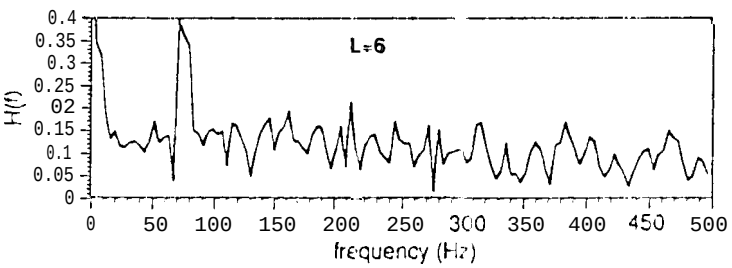
L=6
H(f)
frequency (Hz)

b

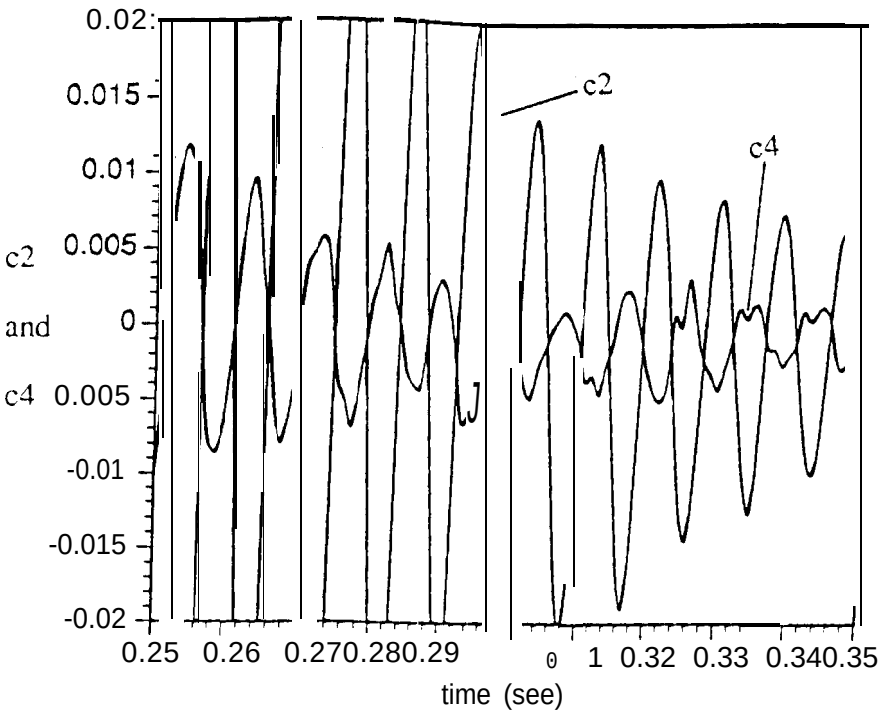

Figure 15.
Superposed plots of the calculated time dependence of the Legendre coefficients c_2 ([) and c_4 (t) at the low amplitude end of the free-clccfiy phase of an oscillating 3 mm diameter water droplet, As the amplitude of the entrained oscillations duc to the fundamental mode c2 (t) decreases, higher frequency components are more apparent. In particular, a component near triple the fundamental mode frequency begins to be more clearly defined with decreasing fundamental mode amplitude.

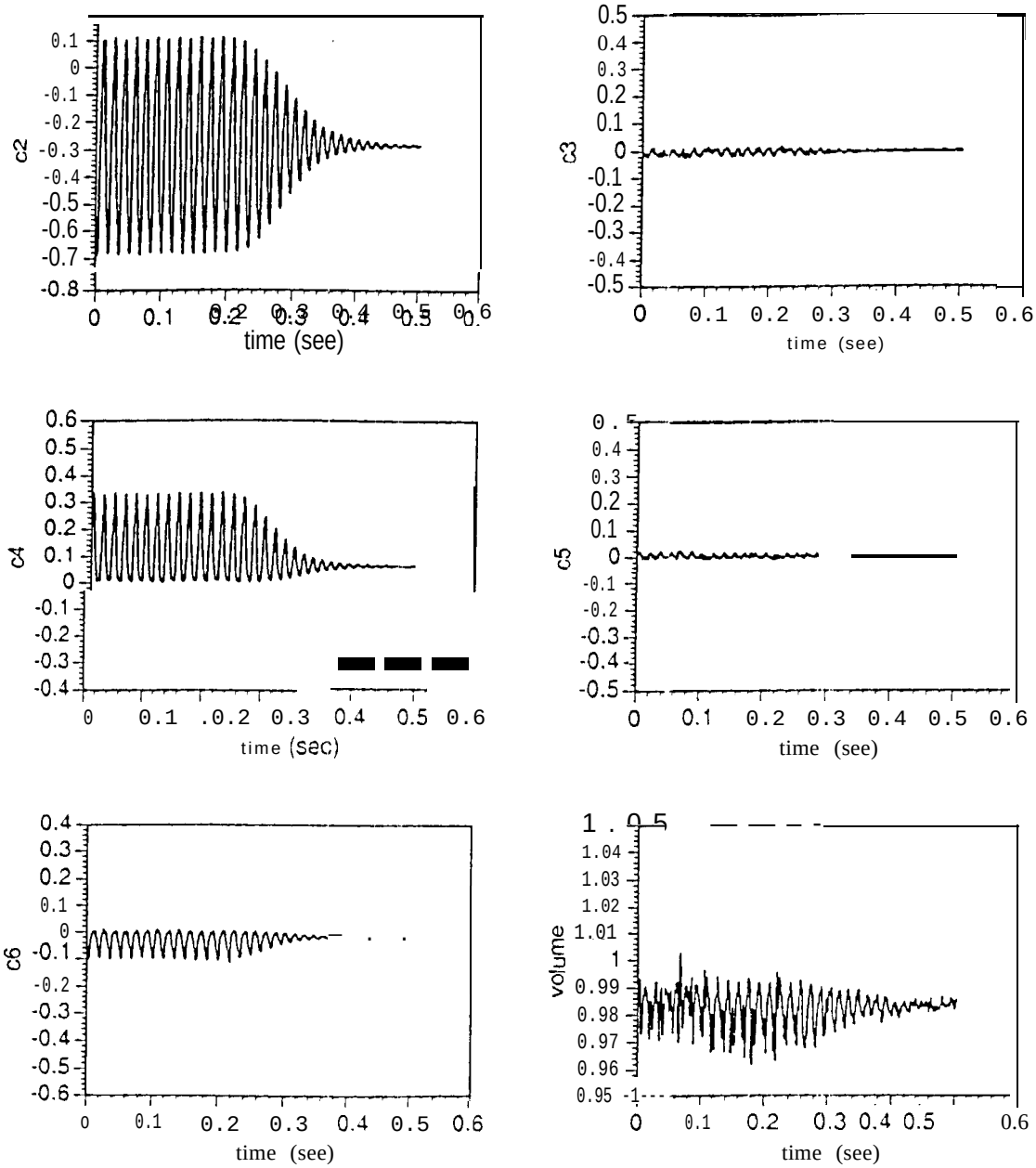

a

Figure **16.**

Time dependence (a) and FFTs (b) of the first five Legendre coefficients of a water-glycerol drop excited into primary resonant oscillations. In [his case the electric force oscillates at 60 H7, and the largest amplitude oscillatory response of the quadrupole mode is at 60 Hz. No odd-numbered oscillations are excited to a significant extent. The decay trace envelope for c 2 (t) is more symmetrical (compared with that in figure 14a) duc to a lesser static drop distortion. 'f he frequency component at 120 Hz for the higher even numbered Legendre coefficients cannot yet be explained.

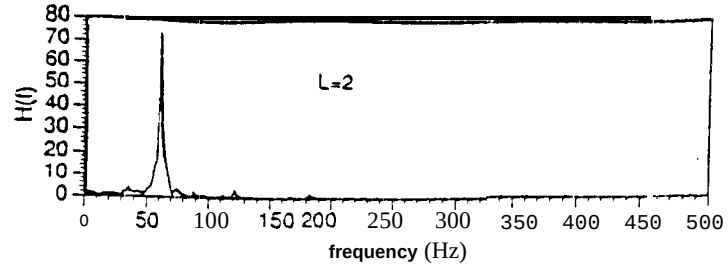
L=2
H(f)
frequency (Hz)

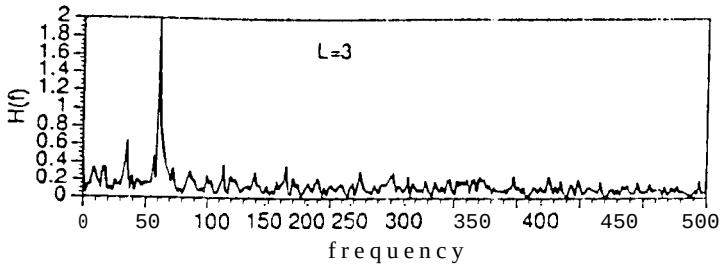
L=3
H(f)
frequency

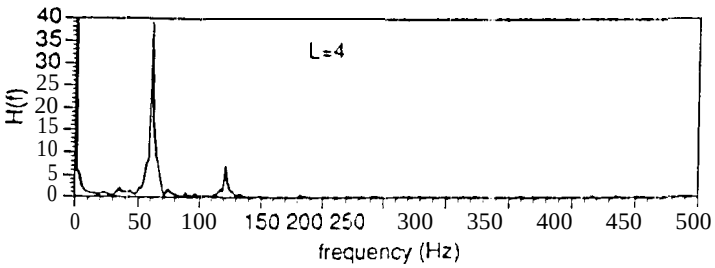
L=4
H(f)
frequency (Hz)

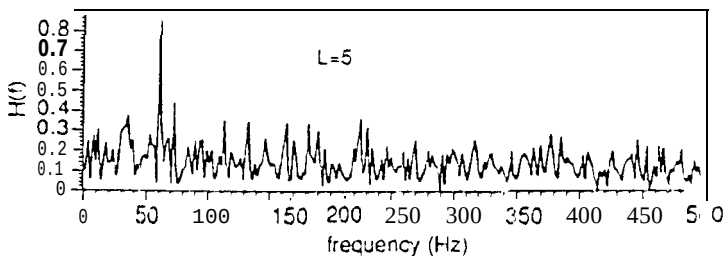
L=5
H(f)
frequency (Hz)

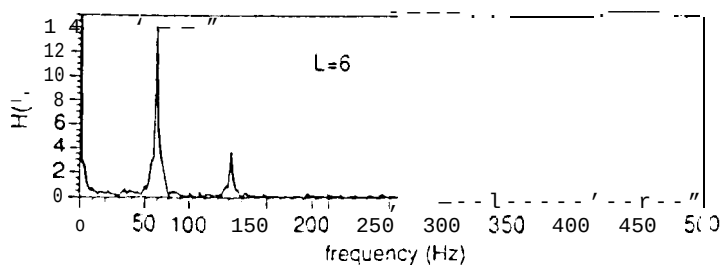
L=6
frequency (Hz)

b

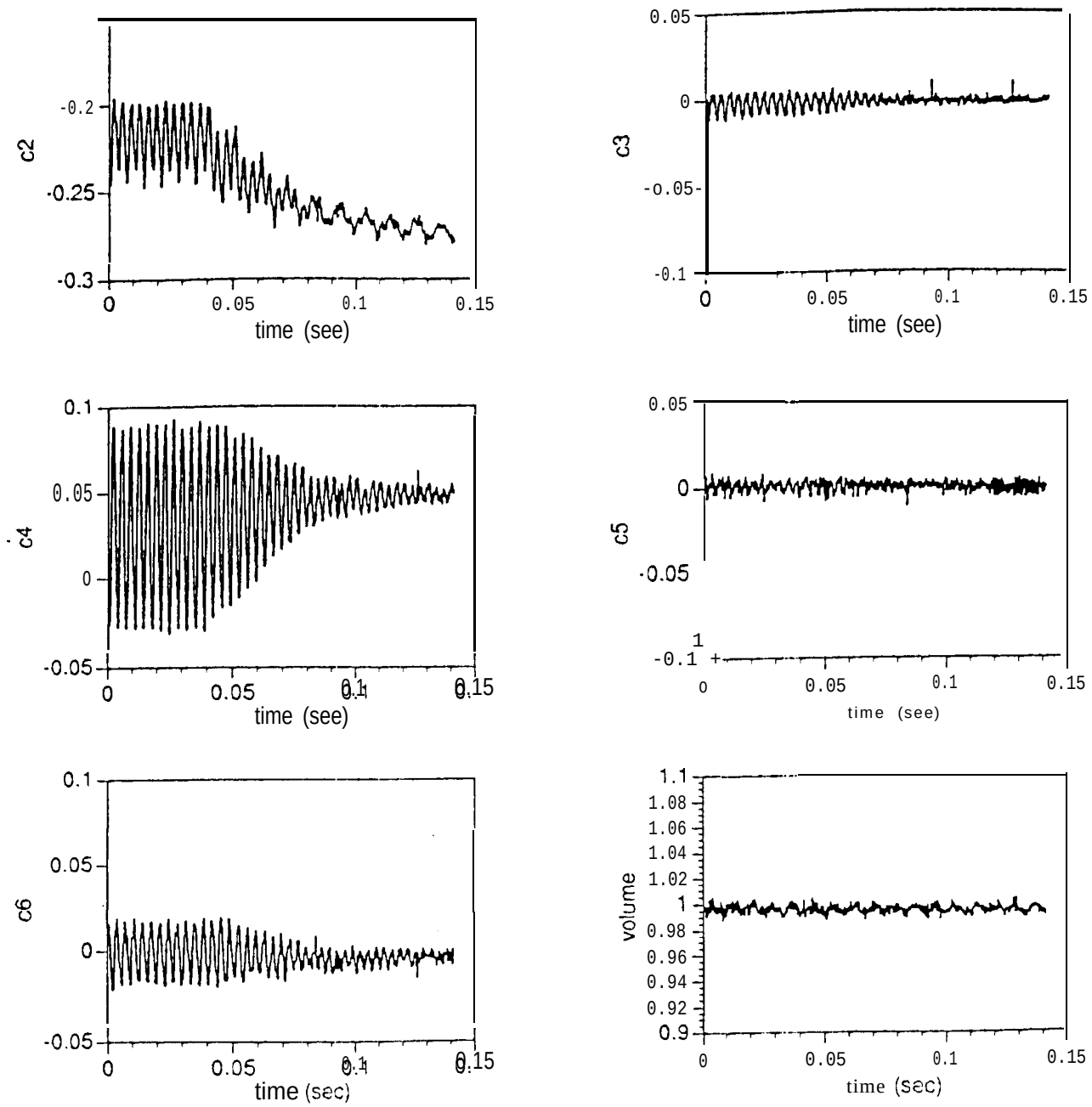

Figure 17.
Time dependence of the first five Legendre coefficients fnr a water droplet in the driven and free-dcc:ty phases. The initial oscillations arc in the l=4 mode, and are directly excited into primary resonance by an electric force oscillating at 143.2 Hz. Fairly large amplitude synchronous oscillations are detected for both l=2 and l=6 sbapcs, as well as a noticeable l=3 component. The natural resonant oscillations of the l:2 mode appear at the end of the decay phase.

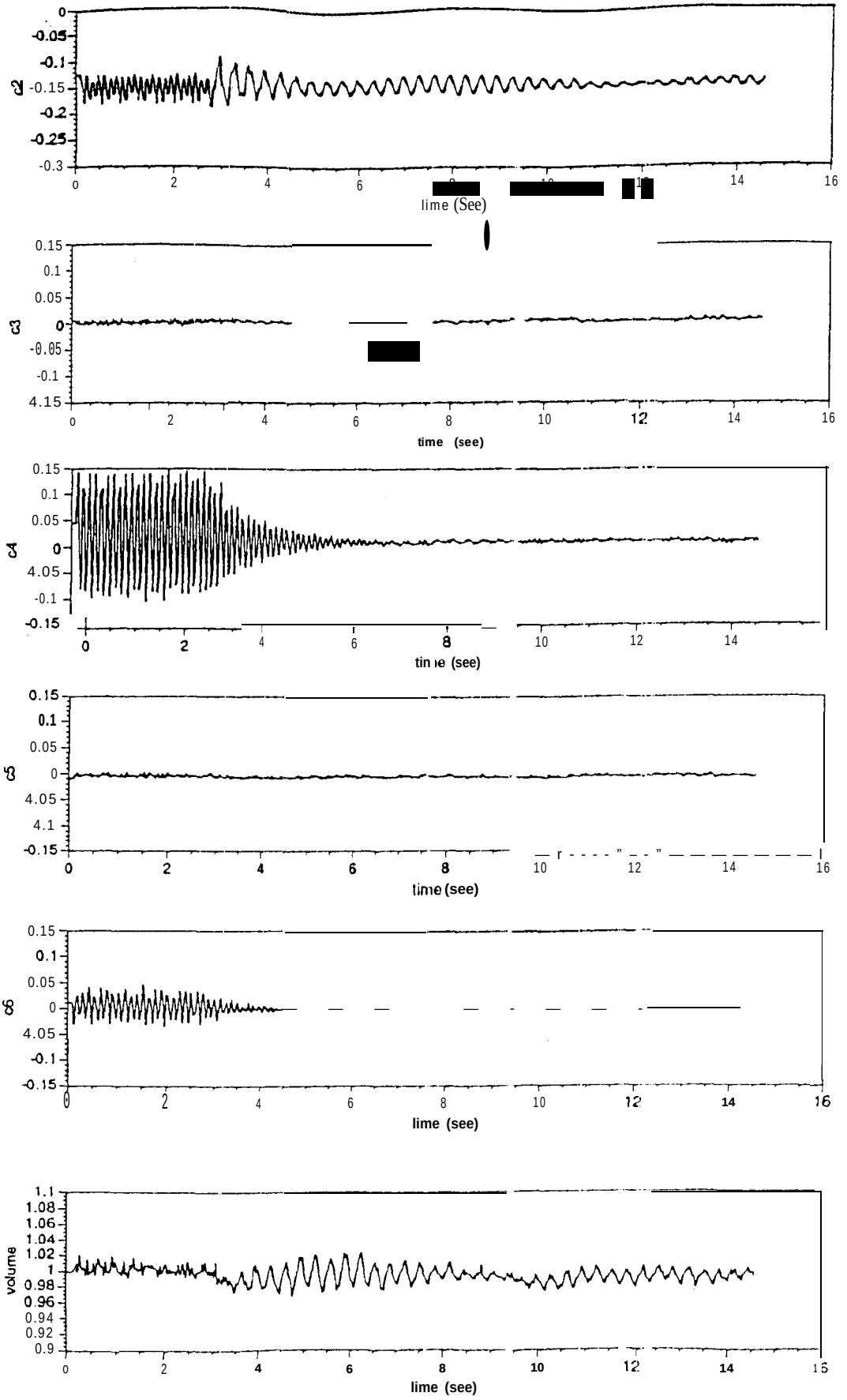

Figure 18.

Time dependence of a first five Legendre coefficients for a rotating water drop acoustically positioned in microgravity. The l=4 mode oscillations are initially excited by modulation of the acoustic radiation pressure, and the free-decay phase is initiated by turning off the amplitude modulation. The equilibrium shape of the drop is slightly oblate (c_2= -(). 15) due to rotation and acoustic radiation stresses. The odd-numbered coefficients response is negligible, **anti** in contrast with the ground-based results, the dominance of the natural frequency of the fundamental mode (l=2) is immediate upon the termination of the l=4 mode drive.

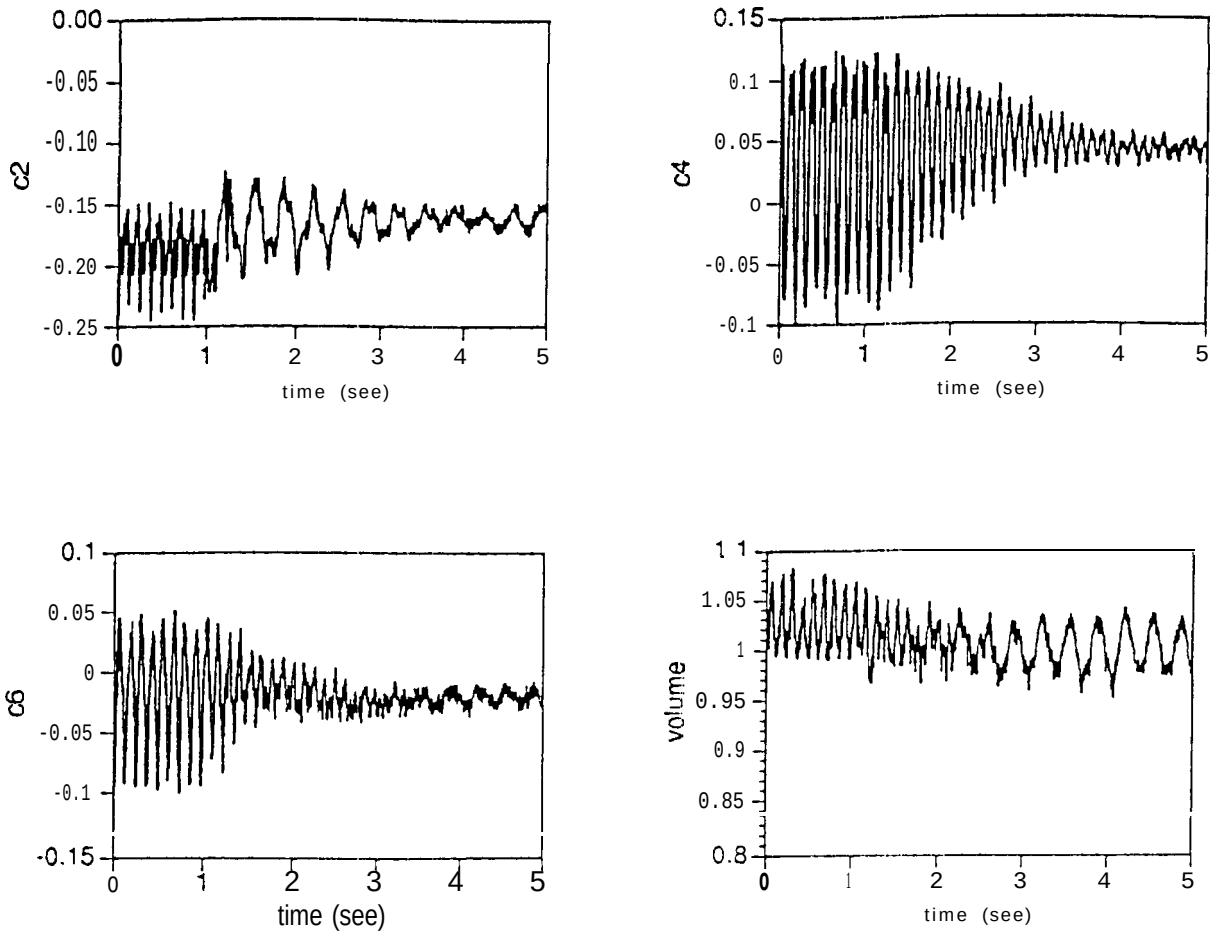

Figure 19.

Results of the analysis of [he driven and free-decay phases of a rotating drop in microgravity and initially driven into the $l=4$ mode oscillations by acoustic radiation pressure modulation. 1 he data were obtained from 16 mm cinefilm records exposed at 400" fr~nws/second. The noisier quality of the data stems from the non-ideal lighting characteristics which create spurious reflections and highlights on the drop images. These results are very similar [o [hose obtained with droplets levitated on Ear[h, except for the earlier appearance of the fundamental natural mode at the onset of free.dcc;iy.